Journal of Industrial and Management Optimization

https://www.aimspress.com/journal/jimo

JIMO, 22(12): 6442–6474.
DOI:10.3934/jimo.2026216
Received: 24 September 2026
Revised: 27 October 2026
Accepted: 04 November 2026
Published: 11 November 2026

Research article

Time-consistent reinsurance-investment game with delay under a multifactor approximation of rough Heston volatility

Yong He[1,*] **and Ga Ba**[2]

[1] School of Mathematical Sciences, Chongqing University of Science and Technology, Chongqing 401331, China

[2] School of Marxism, Southwestern University of Finance and Economics, Chengdu 611130, China

* **Correspondence:** Email: 2007046@cqust.edu.cn.

Abstract: We study a time-consistent reinsurance–investment game between two competing mean–variance insurers under a finite-dimensional approximation of rough Heston volatility. Each insurer controls proportional risk retention and stock investment and evaluates normalized memory-adjusted wealth relative to its competitor. A compatibility condition reduces a restricted class of distributed and point-delay models to a finite-dimensional state with an effective accumulation rate. For the n-factor Markov game, we formulate the joint feedback state, derive the extended HJB system, and prove a verification theorem under explicit fourth-moment and uniform-integrability conditions. The coupled affine best-response equations yield closed-form interior strategies and projected retention controls. Within the affine interior best-response system, we establish uniqueness of the coefficient solution. Reinsurance and investment have different strategic multipliers, $1/(1-\kappa_1\kappa_2\rho_{12}^2)$ and $1/(1-\kappa_1\kappa_2)$, respectively. A matrix-exponential solution retains the aggregate-variance drift coupling and the stock–variance hedging feedback, while common-driver cross-factor covariations enter the generator separately. Under the stated state, terminal-wealth, and local-deviation-gain convergence conditions, a conditional compact-action criterion transfers local-equilibrium inequalities to the original rough game. Numerical experiments compare the rough specification with standard Heston, literal no delay, and a matched-effective-rate benchmark, together with full-interval and truncated-interval kernel-approximation error assessments.

Keywords: reinsurance-investment game; time-consistent Nash equilibrium; rough Heston volatility; multifactor approximation; delay; mean-variance
Mathematics Subject Classification: 91A15, 91G05, 91G10, 93E20

1. Introduction

Insurers must jointly decide how much underwriting risk to retain or transfer and how to allocate assets between risk-free and risky investments. These reinsurance and investment decisions interact because both affect terminal wealth, risk exposure, and solvency under underwriting and financial-market uncertainty. This paper therefore studies the joint reinsurance–investment decisions of competing insurers in a stochastic setting.

To formalize this risk–return trade-off at the insurer level, the decision criterion adopted in this paper is the mean–variance criterion, which captures the insurer's concern for expected terminal wealth and its dispersion. Introduced by Markowitz [1], the mean–variance criterion has become a cornerstone of modern portfolio theory and, more recently, of actuarial decision making. Li and Ng [2] formulated the multiperiod mean–variance portfolio problem in discrete time, whereas Zhou and Li [3] developed its continuous-time stochastic linear–quadratic formulation. In a continuous-time setting, Merton [4] also laid the foundations of dynamic consumption–portfolio choice. Because the mean–variance objective is inherently time-inconsistent, time-consistent equilibrium provides the appropriate decision criterion for a rational insurer; see [5–7] for the general theory and its first application to insurer reinsurance and investment. Building on these advances, an extensive literature now studies the optimal reinsurance–investment problem for a single mean–variance insurer, either with constrained risk control [8], with interest-rate and inflation risks [9], or within a non-zero-sum game against a reinsurer [10]. More recently, the mean-variance reinsurance–investment problem has been solved under stochastic interest rate and volatility [11], and explicit Heston-based optimal investment and proportional reinsurance strategies have been derived [12].

A central recent development is the recognition that insurers do not operate in isolation: They compete with one another for market share and relative performance. When each insurer also cares about its wealth *relative to* that of its competitor, the natural formulation is a non-zero-sum stochastic differential game whose equilibrium is a Nash equilibrium. The theory of such relative-performance concerns was initiated in fund management [13] and optimal investment [14], and was then brought into insurance games [10,15]. Explicit Nash equilibria were subsequently derived for two constant absolute risk aversion (CARA) insurers with default risk and relative-performance concerns [16]. The time inconsistency induced by the mean–variance objective interacts nontrivially with this competition, and the resulting equilibrium strategies can depart substantially from the single-agent optimum [17]. Recent developments extend this line to multiple mean-variance insurers with mispricing and default risks [18], to dependent claim structures [19], and to data-driven non-zero-sum games solved within a reinforcement-learning framework [20].

The closest benchmarks clarify the remaining gap. Existing studies derive time-consistent investment and reinsurance strategies under the standard Heston model [21], formulate a robust non-zero-sum game with default risk [22], and combine model uncertainty with time-consistent mean–variance competition [23]. These studies establish the strategic relative-performance channel, but they do not combine normalized wealth memory with the common-driver multifactor lift of rough Heston volatility. Conversely, rough-volatility portfolio studies do not include strategic proportional reinsurance. This paper constructs a tractable game that combines normalized wealth memory, a common-driver multifactor lift of rough Heston volatility, and strategic proportional reinsurance within a compatible delay subclass.

Two modeling features remain difficult to combine with competitive mean–variance control. First, capital distributions may depend on past wealth. This dependence leads to stochastic delay equations with

both distributed and pointwise memory. A finite-dimensional reduction is available under a compatibility condition [24], while delay also changes asset-pricing dynamics [25]. Delay has further been incorporated into hybrid reinsurance–investment games [26], robust mean–variance models [27], and Stackelberg games with bounded memory [28]. Second, equity volatility is empirically rough [29]. The rough Heston variance is non-Markovian and therefore does not directly support the finite-dimensional extended Hamilton–Jacobi–Bellman (HJB) analysis used for time-consistent games. Relevant approaches include the rough Heston model [30], multifactor approximation [31], Markovian lifting [32], and rough-volatility portfolio optimization [33]. Multifactor constructions have also been used for rough Hawkes–Heston models [34], while control convergence has been analyzed in a hedging problem [35].

The unresolved issue is therefore not the absence of any one ingredient. It is the construction of a tractable equilibrium when time inconsistency, competition, delay, and a common-driver rough-volatility approximation act together. The closest insurance-game studies do not include the coupled rough-volatility factor system, while existing rough-volatility portfolio studies do not address strategic reinsurance and relative performance. The common volatility driver is technically important because it creates cross-factor covariations. Treating the factors as independent scalar equations would change both the generator and the investment hedge.

We address this issue through a finite-dimensional multifactor approximation of rough Heston volatility. The closed-form analysis concerns the resulting n-factor Markov game. Under uniform convergence of local-deviation gains, a separate conditional transfer criterion carries the finite-factor local-equilibrium inequalities to the original rough game.

The main innovations of this paper are as follows.

(i) We formulate a path-dependent reinsurance–investment game for two mean–variance insurers. A signed performance-linked cash-flow rule uses both a normalized exponentially weighted average $M_k(t)$ and the pointwise lag $N_k(t)$. The compatibility condition defines a restricted parameter subclass in which these delay variables enter the control problem through memory-adjusted relative wealth and an effective accumulation rate.

(ii) We replace rough volatility by a nonnegative n-factor Markovian lift and define the associated joint-state feedback and spike-deviation classes. We derive the extended HJB system and prove a verification theorem for this finite-factor game. Under explicit state, terminal-wealth, and local-deviation-gain stability conditions, a separate compact-action lemma transfers local equilibrium inequalities to the original rough game.

(iii) We solve the coupled affine best-response equations in closed form for interior retentions and establish uniqueness of the coefficient solution within the affine interior best-response system; for boundary solutions, we provide a projected system. Among the two correlation channels, reinsurance depends on ρ_{12} through $1/(1-\kappa_1\kappa_2\rho_{12}^2)$, whereas investment depends on ρ_{sv} and is coupled through $1/(1-\kappa_1\kappa_2)$. The matrix coefficient separates the aggregate-variance drift and hedging feedback from the cross-factor second-order covariations generated by the common volatility driver.

(iv) We conduct numerical experiments using parameter values informed by published rough-volatility estimates. The experiments distinguish the two correlation channels, quantify relative performance, and compare the rough specification with standard Heston, literal no delay, and no delay at a

matched effective accumulation rate. Full-interval and truncated-interval kernel-approximation error assessments distinguish finite-factor agreement from approximation of the rough kernel.

The remainder of the paper is organized as follows. Section 2 formulates the problem: It describes the rough Heston market, the delayed wealth dynamics, and the mean–variance optimization problem. Section 3 introduces the multifactor approximation and a conditional equilibrium-transfer criterion. Section 4 derives the verification theorem and the closed-form Nash equilibrium strategies together with their value functions. Section 5 presents numerical experiments and their economic interpretation. Concluding remarks follow.

2. Problem formulation

In this section, we formulate the reinsurance–investment game problem between two competing mean–variance insurers whose wealth processes are driven by a rough Heston stock and a stochastic delay. Assume that all stochastic variables and stochastic processes involved in this paper are well defined on a complete probability space $(\Omega, \mathcal{F}, \{\mathcal{F}_t\}_{0\le t\le T}, \mathbb{P})$, which satisfies the usual conditions ($\{\mathcal{F}_t\}_{0\le t\le T}$ is right-continuous and $\mathbb{P}$-complete). Trading is continuous and frictionless over the finite horizon $[0, T]$. Throughout, $k, j \in \{1, 2\}$ and $k \neq j$ unless stated otherwise.

Consider two competing insurers. Before reinsurance and investment, insurer k's surplus satisfies

$$\mathrm{d}R_k(t) = \mu_k\,\mathrm{d}t + \sigma_k\,\mathrm{d}B_k(t), \tag{1}$$

where the constants μ_k and $\sigma_k > 0$ are the premium income rate and volatility, respectively. The standard Brownian motions $B_1(t)$ and $B_2(t)$ satisfy $\mathrm{d}\langle B_1, B_2\rangle_t = \rho_{12}\,\mathrm{d}t$ and are independent of $W_s(t)$ and $W_v(t)$ appearing in (3) and (4).

Insurer k controls risk through proportional reinsurance and seeks additional return through investment. Let $a_k(t) \in [0, 1]$ be its retained fraction at time t. The fraction $1 - a_k(t)$ is ceded to the reinsurer at premium rate $(1 - a_k(t))\eta_k$, where $\eta_k \ge \mu_k$. Under this convention, the controlled surplus satisfies

$$\mathrm{d}R_k(t) := [\theta_k + \eta_k a_k(t)]\mathrm{d}t + \sigma_k a_k(t)\,\mathrm{d}B_k(t), \tag{2}$$

where $\theta_k = \mu_k - \eta_k$ is the premium difference. For the investment, we assume that the insurer can divide its assets between a risk-free bond and a risky stock. The risk-free rate is $r_f > 0$, and the risky asset price $S(t)$ satisfies the rough Heston model

$$\frac{\mathrm{d}S(t)}{S(t)} = (r_f + mv(t))\,\mathrm{d}t + \sqrt{v(t)}\,\mathrm{d}W_s(t), \qquad S(0) = s(0) > 0, \tag{3}$$

in which the volatility process $v(t)$ is given by

$$v(t) = v(0) + \int_0^t K(t-s)\Big[\kappa(\omega - v(s))\,\mathrm{d}s + \sigma_v\sqrt{v(s)}\,\mathrm{d}W_v(s)\Big], \qquad v(0) = v_0 > 0, \tag{4}$$

where m is the variance-risk premium, κ, ω, and σ_v are positive constants, and $K(t)$ is the kernel function

$$K(t) = \frac{t^{H-1/2}}{\Gamma(H + 1/2)} \tag{5}$$

with Hurst index $H \in (0, 1/2)$. The standard Brownian motions $W_s(t)$ and $W_v(t)$ have stock–variance correlation $-1 \le \rho_{sv} \le 1$, i.e., $\mathrm{d}\langle W_s(t), W_v(t)\rangle = \rho_{sv}\,\mathrm{d}t$, and are used to describe the uncertainty of stock process and variance process, respectively.

Assume that each k-th insurer can dynamically provide new insurance business, purchase proportional reinsurance, and adjust investment level in the stock. Let $b_k(t)$ be the money amount that the k-th insurer invests in the stock, and the rest is invested in the risk-free bond. Therefore, the wealth dynamics of insurer k, denoted by $X_k^\pi(t)$, evolves as

$$\begin{aligned}\mathrm{d}X_k^\pi(t) = {} & [r_f X_k^\pi(t) + \theta_k + \eta_k a_k(t) + m b_k(t) v(t)]\,\mathrm{d}t \\ & + \sigma_k a_k(t)\,\mathrm{d}B_k(t) + b_k(t)\sqrt{v(t)}\,\mathrm{d}W_s(t),\end{aligned} \tag{6}$$

where $\pi_k(t) := (a_k(t), b_k(t))$, with the admissible path-dependent strategy class defined after the delay state has been specified.

To incorporate past information, define the normalization constant $q_\delta = \delta/(1-e^{-\delta h})$ and two processes $M_k(t)$ and $N_k(t)$ by

$$M_k(t) = q_\delta \int_{-h}^{0} e^{\delta u} X_k(t+u)\,\mathrm{d}u, \qquad N_k(t) = X_k(t-h), \tag{7}$$

which represent the normalized exponentially weighted average and the pointwise delayed wealth over $[t-h, t]$, respectively. The normalization gives $M_k(t) = x$ whenever $X_k(s) \equiv x$ on the memory window, so $X_k - M_k$ has the same units as wealth and vanishes for a constant history. Here $\delta > 0$ is the decay rate, and $h > 0$ is the delay length. Differentiating the integral using the argument in Lemma 3.1 [24] gives

$$\mathrm{d}M_k(t) = \left(q_\delta X_k(t) - \delta M_k(t) - q_\delta e^{-\delta h} N_k(t)\right)\mathrm{d}t. \tag{8}$$

Let $G_k(t)$ denote a *signed rate of capital distribution*. Positive $G_k(t)$ represents a withdrawal from the insurer, such as a dividend or a transfer to policyholders, whereas negative $G_k(t)$ represents a capital injection. We link that rate to two performance gaps, the deviation of current wealth from its exponentially weighted history and the deviation from the pointwise lag:

$$\begin{aligned}G_k(t) &= \alpha_k(X_k(t) - M_k(t)) + \beta_k(X_k(t) - N_k(t)) \\ &= (\alpha_k + \beta_k)X_k(t) - \alpha_k M_k(t) - \beta_k N_k(t),\end{aligned} \tag{9}$$

where α_k and β_k are nonnegative sensitivity coefficients. The minus sign in equation (10) follows the stated sign convention. If current wealth exceeds either historical benchmark, the corresponding positive gap produces an outflow; if current wealth is below its benchmark, the term is negative, and $-G_k(t)\,\mathrm{d}t$ becomes an inflow. Thus the construction specifies a mean-reverting performance-linked cash-flow rule. We assume $\alpha_1 = \alpha_2 =: \alpha$ and $\beta_1 = \beta_2 =: \beta$ so that the same memory rule applies to both insurers.

We retain the notation $X_k^\pi(t)$ for the delayed wealth process, which is governed by

$$\begin{aligned}\mathrm{d}X_k^\pi(t) = {} & [r_f X_k^\pi(t) + \theta_k + \eta_k a_k(t) + m b_k(t) v(t) - G_k(t)]\,\mathrm{d}t \\ & + \sigma_k a_k(t)\,\mathrm{d}B_k(t) + b_k(t)\sqrt{v(t)}\,\mathrm{d}W_s(t).\end{aligned} \tag{10}$$

Combining with (9), we can rewrite (10) as

$$\begin{aligned}\mathrm{d}X_k^\pi(t) = {} & [r_1 X_k^\pi(t) + \alpha M_k(t) + \beta N_k(t) + \theta_k + \eta_k a_k(t) + m b_k(t) v(t)]\,\mathrm{d}t \\ & + \sigma_k a_k(t)\,\mathrm{d}B_k(t) + b_k(t)\sqrt{v(t)}\,\mathrm{d}W_s(t),\end{aligned} \tag{11}$$

where $r_1 = r_f - \alpha - \beta$.

Since the two insurers compete with each other, they consider seeking an admissible reinsurance and investment strategy π_k to maximize the utility of relative wealth. Following [14], we define the relative wealth of the k-th insurer denoted by $Z_k^{(\pi_k,\pi_j)}(t)$ as

$$\begin{aligned} Z_k^{(\pi_k,\pi_j)}(t) &= (1-\kappa_k)X_k^{\pi}(t) + \kappa_k(X_k^{\pi}(t) - X_j^{\pi}(t)) \\ &= X_k^{\pi}(t) - \kappa_k X_j^{\pi}(t), \end{aligned} \tag{12}$$

where $\kappa_k \in [0,1]$ measures insurer k's sensitivity to the performance of its competitor. A larger κ_k assigns greater weight to relative performance and represents a stronger concern for relative wealth.

Using Itô's formula in (12), the relative wealth of insurer k satisfies

$$\begin{cases} \mathrm{d}Z_k^{(\pi_k,\pi_j)}(t) = \mathrm{d}X_k^{\pi}(t) - \kappa_k \mathrm{d}X_j^{\pi}(t) \\ \quad = \Big[r_1 Z_k^{(\pi_k,\pi_j)}(t) + \alpha(M_k(t) - \kappa_k M_j(t)) + \beta(N_k(t) - \kappa_k N_j(t)) \\ \qquad +(\theta_k - \kappa_k\theta_j) + (\eta_k a_k(t) - \kappa_k \eta_j a_j(t)) + m(b_k(t) - \kappa_k b_j(t))v(t) \Big] \mathrm{d}t \\ \qquad +\sigma_k a_k(t)\,\mathrm{d}B_k(t) - \kappa_k\sigma_j a_j(t)\,\mathrm{d}B_j(t) + (b_k(t) - \kappa_k b_j(t))\sqrt{v(t)}\,\mathrm{d}W_s(t), \\ Z_k^{(\pi_k,\pi_j)}(0) = z_k = x_k - \kappa_k x_j. \end{cases} \tag{13}$$

Write $Y_k(t) = M_k(t) - \kappa_k M_j(t)$. Then (13) becomes

$$\begin{aligned} \mathrm{d}Z_k^{(\pi_k,\pi_j)}(t) = \Big[& r_1 Z_k^{(\pi_k,\pi_j)}(t) + \alpha Y_k(t) + \beta(N_k(t) - \kappa_k N_j(t)) \\ & + (\theta_k - \kappa_k\theta_j) + (\eta_k a_k(t) - \kappa_k \eta_j a_j(t)) + m(b_k(t) - \kappa_k b_j(t))v(t) \Big] \mathrm{d}t \\ & + \sigma_k a_k(t)\,\mathrm{d}B_k(t) - \kappa_k\sigma_j a_j(t)\,\mathrm{d}B_j(t) + (b_k(t) - \kappa_k b_j(t))\sqrt{v(t)}\,\mathrm{d}W_s(t), \end{aligned} \tag{14}$$

where $Y_k(t)$ satisfies

$$\mathrm{d}Y_k(t) = [q_\delta Z_k(t) - \delta Y_k(t) - q_\delta e^{-\delta h}(N_k(t) - \kappa_k N_j(t))]\,\mathrm{d}t. \tag{15}$$

To obtain a finite-dimensional state for the subsequent HJB analysis, we impose the standard compatibility condition for distributed and pointwise delay. Let $\chi > 0$ satisfy

$$\beta = \chi q_\delta e^{-\delta h}, \qquad \alpha - \chi\delta = \bar{r}\chi, \qquad \bar{r} := r_1 + \chi q_\delta. \tag{16}$$

Define the memory-adjusted relative wealth

$$\bar{Z}_k(t) := Z_k(t) + \chi Y_k(t). \tag{17}$$

Combining (13), (15), and (16) cancels the pointwise lag $N_k(t) - \kappa_k N_j(t)$ and yields

$$\begin{aligned} \mathrm{d}\bar{Z}_k(t) = \Big[& \bar{r}\bar{Z}_k(t) + (\theta_k - \kappa_k\theta_j) + \eta_k a_k(t) - \kappa_k\eta_j a_j(t) \\ & + m(b_k(t) - \kappa_k b_j(t))v(t) \Big] \mathrm{d}t \\ & + \sigma_k a_k(t)\,\mathrm{d}B_k(t) - \kappa_k\sigma_j a_j(t)\,\mathrm{d}B_j(t) + (b_k(t) - \kappa_k b_j(t))\sqrt{v(t)}\,\mathrm{d}W_s(t). \end{aligned} \tag{18}$$

Condition (16) defines the compatible delay subclass. It links the two cash-flow sensitivities to the memory loading, cancels the pointwise lag, and combines the coefficients of Z_k and Y_k into $\bar{r}\bar{Z}_k$. The resulting finite-dimensional HJB state yields the explicit equilibrium, and the distributed and point-delay responses are jointly determined within this parameterization. Economically, this subclass describes a single performance-linked cash-flow mechanism whose distributed-memory and point-lag responses are calibrated jointly. Once (χ, δ, h, r_f) is fixed, the two compatibility relations determine β and α, and thereby determine the effective accumulation rate $\bar{r}$. The compatible subclass represents jointly calibrated, rather than independently chosen, values of α, β, and χ. Outside this subclass, the point-lag term remains in the state dynamics and requires an augmented path-state analysis beyond the finite-dimensional reduction used below.

For the numerical experiments, insurer k is endowed with initial wealth x_k and has the constant prehistory $X_k(s) = x_k$ for $s \in [-h, 0]$. Accordingly, $M_k(0) = N_k(0) = x_k$ by (7).

Definition 1. *Let $\mathbb{U}_k = [0,1] \times \mathbb{R}$ be insurer k's action set and let $\mathcal{H}_t = C([t-h, t]; \mathbb{R}^2)$ collect the two wealth histories. A strategy $\pi_k = \{(a_k(s), b_k(s))\}_{s\in[t,T]}$ is admissible from $(\boldsymbol{x}_t, \mathcal{V}_t) \in \mathcal{H}_t \times C([0,t]; \mathbb{R}_+)$ if it is non-anticipative and $\mathcal{F}_s$-progressively measurable, takes values in $\mathbb{U}_k$, and satisfies*

$$\mathbb{E}_t\left[\int_t^T |b_k(s)|^4 \, \mathrm{d}s\right] < \infty. \tag{19}$$

For every admissible initial history, the delayed wealth system (10) *must have a pathwise unique solution, and the fourth-moment bound*

$$\mathbb{E}_t\left[\sup_{s\in[t,T]} (|X_1(s)|^4 + |X_2(s)|^4)\right] < \infty \tag{20}$$

must hold. This order is sufficient for the quadratic terminal criterion, the stopped Itô arguments, and the spike remainder used below. The corresponding strategy class is denoted by Π_k. The dependence on the wealth history and on $\mathcal{V}_t$ is suppressed when no confusion can arise.

Each insurer evaluates the terminal memory-adjusted relative wealth by a mean–variance criterion. Let $\mathcal{V}_t := \{v(s) : 0 \le s \le t\}$ denote the observed rough-volatility history. The objective is

$$J_k^{(\pi_k, \pi_j^*)}(t, z_k, y_k; \mathcal{V}_t) := \mathbb{E}_t\left[\bar{Z}_k^{(\pi_k,\pi_j^*)}(T)\right] - \frac{\gamma_k}{2}\mathrm{Var}_t\left[\bar{Z}_k^{(\pi_k,\pi_j^*)}(T)\right], \tag{21}$$

where $\pi_j^* := (a_j^*, b_j^*)$, $\gamma_k > 0$ is the risk-aversion coefficient and $\mathbb{E}_t[\cdot] = \mathbb{E}[\cdot \mid \mathcal{F}_t]$. The arguments $(z_k, y_k; \mathcal{V}_t)$ record the current delay variables and the full volatility history. In particular, conditioning only on the scalar $v(t)$ would not describe the state of the rough model. By (18), the delay variables enter the continuation problem through $\bar{z}_k = z_k + \chi y_k$.

$$F_k(y) = y - \frac{\gamma_k}{2}y^2, \qquad H_k(y) = \frac{\gamma_k}{2}y^2. \tag{22}$$

Then (21) can be rewritten as

$$J_k^{(\pi_k,\pi_j^*)} = \mathbb{E}_t\left[F_k\left(\bar{Z}_k^{(\pi_k,\pi_j^*)}(T)\right)\right] + H_k\left(\mathbb{E}_t\left[\bar{Z}_k^{(\pi_k,\pi_j^*)}(T)\right]\right). \tag{23}$$

Because the mean–variance criterion is time-inconsistent, we define equilibrium through local deviations. Fix $t < T$, $0 < \epsilon < T - t$, and a bounded action $u_k = (\widetilde{a}_k, \widetilde{b}_k) \in \mathbb{U}_k$. With the opponent kept at π_j^*, define the spike policy

$$\pi_k^{t,\epsilon;u_k}(s) := \begin{cases} u_k, & t \le s < t + \epsilon, \\ \pi_k^*(s), & t + \epsilon \le s \le T. \end{cases} \tag{24}$$

The second branch is evaluated at the state and history generated by the first. Thus the deviating and equilibrium policies are distinct whenever $u_k \neq \pi_k^*(t)$. The pair $(\pi_1^*, \pi_2^*) \in \Pi_1 \times \Pi_2$ is a time-consistent Nash equilibrium if, for $k \neq j$, every bounded $u_k \in \mathbb{U}_k$, and every admissible initial history at t,

$$\liminf_{\epsilon \downarrow 0} \frac{J_k^{(\pi_k^*, \pi_j^*)}(t, z_k, y_k; \mathcal{V}_t) - J_k^{(\pi_k^{t,\epsilon;u_k}, \pi_j^*)}(t, z_k, y_k; \mathcal{V}_t)}{\epsilon} \ge 0. \tag{25}$$

The associated equilibrium value is $J_k^{(\pi_k^*, \pi_j^*)}(t, z_k, y_k; \mathcal{V}_t)$.

3. Multifactor approximation

The rough variance history prevents a finite-dimensional HJB treatment of (21). We therefore use the multifactor construction in [31]. This construction replaces the fractional kernel by a positive exponential sum and yields the Markovian system

$$\frac{\mathrm{d}S_n(t)}{S_n(t)} = (r_f + m v_n(t))\,\mathrm{d}t + \sqrt{v_n(t)}\,\mathrm{d}W_s(t), \tag{26}$$

$$v_n(t) = g_n(t) + \sum_{i=1}^{n} c_{n,i}\, v_{n,i}(t), \tag{27}$$

$$\mathrm{d}v_{n,i}(t) = (-\gamma_{n,i} v_{n,i}(t) - \kappa v_n(t))\,\mathrm{d}t + \sigma_v \sqrt{v_n(t)}\,\mathrm{d}W_v(t), \qquad i = 1, \dots, n, \qquad v_{n,i}(0) = 0, \tag{28}$$

where

$$g_n(t) = v(0) + \kappa\omega \int_0^t \sum_{i=1}^{n} c_{n,i} e^{-\gamma_{n,i}(t-s)}\,\mathrm{d}s \tag{29}$$

and the Bernstein measure of the fractional kernel is

$$\mu_H(\mathrm{d}\gamma) = \frac{\gamma^{-H-1/2}}{\Gamma(H + \frac{1}{2})\Gamma(\frac{1}{2} - H)}\,\mathrm{d}\gamma, \qquad 0 < H < \tfrac{1}{2}. \tag{30}$$

For fixed truncation points $0 < \underline{\eta} < \overline{\eta} < \infty$, we use the moment-matched quadrature

$$\begin{aligned} c_{n,i} &= \int_{\eta_{n,i-1}}^{\eta_{n,i}} \mu_H(\mathrm{d}\gamma), \\ \gamma_{n,i} &= \frac{1}{c_{n,i}} \int_{\eta_{n,i-1}}^{\eta_{n,i}} \gamma\, \mu_H(\mathrm{d}\gamma), \end{aligned} \qquad i = 1, \dots, n, \tag{31}$$

with

$$\eta_{n,i} = \left[\underline{\eta}^{1/2-H} + \frac{i}{n} \left(\overline{\eta}^{1/2-H} - \underline{\eta}^{1/2-H} \right) \right]^{1/(1/2-H)}, \qquad i = 0, 1, \dots, n. \tag{32}$$

Thus the cells have equal μ_H-mass, and $\gamma_{n,i}$ is the first-moment representative of cell i. The resulting approximate kernel is

$$K_n(t) = \sum_{i=1}^{n} c_{n,i} e^{-\gamma_{n,i} t}. \tag{33}$$

Remark 1. *The model in* (26)–(28) *has one Heston-type factor when* $n = 1$. *For fixed* $[\underline{\eta}, \overline{\eta}]$, *increasing* n *converges only to the truncated kernel. Approximation of the full fractional kernel additionally requires a sequence* $\underline{\eta}_n \downarrow 0$ *and* $\overline{\eta}_n \uparrow \infty$ *such that* $K_n \to K$ *in the norm required by the stability result; see Theorem 3.5 in [31]. Section 5 therefore reports separate assessments of factor-refinement convergence and truncation-range expansion.*

Write $\boldsymbol{v}_n = (v_{n,1}, \ldots, v_{n,n})$ and

$$v_n(t, \boldsymbol{v}_n) = g_n(t) + \sum_{i=1}^{n} c_{n,i} v_{n,i}. \tag{34}$$

For a factor state observed at time t, define the associated forward input curve

$$g^{(n)}_{t,\boldsymbol{v}}(s) := g_n(t+s) + \sum_{i=1}^{n} c_{n,i} e^{-\gamma_{n,i} s} v_i, \qquad 0 \le s \le T - t, \tag{35}$$

and let $\mathcal{G}_{K_n}$ denote the admissible input-curve class for the kernel K_n in Appendix B of [31]. This class is defined through the resolvent-of-the-first-kind shift condition used in their nonnegativity theorem; pointwise nonnegativity of an input curve alone is not its definition. We therefore take the viable factor set to be

$$\mathcal{V}_n(t) := \{\boldsymbol{v} \in \mathbb{R}^n : g^{(n)}_{t,\boldsymbol{v}} \in \mathcal{G}_{K_n} \text{ on } [0, T-t]\}. \tag{36}$$

This condition is stronger than requiring only $g^{(n)}_{t,\boldsymbol{v}}(s) \ge 0$. In particular, $\mathcal{V}_n(t)$ is generally smaller than the half-space $\{\boldsymbol{v} : v_n(t, \boldsymbol{v}) > 0\}$, and individual factor coordinates may be negative even when the aggregate variance is nonnegative.

Lemma 1. *Suppose that* $c_{n,i} > 0$, $\gamma_{n,i} \ge 0$, $\kappa \ge 0$, $\sigma_v \ge 0$, *and* $v_0, \omega \ge 0$. *Then* K_n *is a nonnegative smooth completely monotone kernel and*

$$g_n(t) = v_0 + (K_n * \xi)(t), \qquad \xi(\mathrm{d}s) = \kappa\omega \, \mathrm{d}s \tag{37}$$

belongs to $\mathcal{G}_{K_n}$. *Consequently,* (27)–(28) *has a unique continuous strong solution with* $v_n(t) \ge 0$ *on* $[0, T]$. *Moreover, for every* $p \ge 2$,

$$\sup_{0 \le s \le T} \mathbb{E}[v_n^p(s)] < \infty. \tag{38}$$

For any admissible initial state, the shifted input curve $g^{(n)}_{t,\boldsymbol{v}_n(t)}$ *remains in* $\mathcal{G}_{K_n}$ *almost surely, so* $\boldsymbol{v}_n(t) \in \mathcal{V}_n(t)$.

Proof. For every integer $q \ge 0$ and $t \ge 0$,

$$(-1)^q K_n^{(q)}(t) = \sum_{i=1}^{n} c_{n,i} \gamma_{n,i}^q e^{-\gamma_{n,i} t} \ge 0. \tag{39}$$

Thus K_n is C^∞, nonnegative, and completely monotone. Moreover,

$$(K_n * \xi)(t) = \kappa\omega \int_0^t \sum_{i=1}^n c_{n,i} e^{-\gamma_{n,i}(t-s)}\, \mathrm{d}s = g_n(t) - v_0. \tag{40}$$

Since $v_0 \geq 0$ and ξ is a nonnegative measure, the resolvent-of-the-first-kind criterion in Remark B.6 of [31] yields $g_n \in \mathcal{G}_{K_n}$.

Variation of constants in (28) gives

$$v_{n,i}(t) = -\kappa \int_0^t e^{-\gamma_{n,i}(t-s)} v_n(s)\, \mathrm{d}s + \sigma_v \int_0^t e^{-\gamma_{n,i}(t-s)} \sqrt{v_n(s)}\, \mathrm{d}W_v(s). \tag{41}$$

Multiplication by $c_{n,i}$, summation over i, and use of (27) yield the scalar Volterra equation

$$v_n(t) = g_n(t) - \kappa \int_0^t K_n(t-s) v_n(s)\, \mathrm{d}s + \sigma_v \int_0^t K_n(t-s) \sqrt{v_n(s)}\, \mathrm{d}W_v(s). \tag{42}$$

Theorem B.4 of [31], applied to the admissible input g_n, gives a nonnegative weak solution of (42). Because K_n is smooth and $x \mapsto \sigma_v \sqrt{x^+}$ is 1/2-Hölder, Proposition B.3 therein gives pathwise uniqueness. Hence the weak solution is strong and unique. By Proposition B.1 therein, for each $p \geq 2$ there is a finite constant $C_{p,T}$ such that

$$\sup_{0 \leq s \leq T} \mathbb{E}[v_n^p(s)] \leq C_{p,T}, \tag{43}$$

which is (38).

Finally, fix $t \in [0, T]$. Applying the preceding variation-of-constants identity from t to $t + s$ gives, for $0 \leq s \leq T - t$,

$$\begin{aligned} v_n(t+s) = g^{(n)}_{t,\boldsymbol{v}_n(t)}(s) &- \kappa \int_0^s K_n(s-r) v_n(t+r)\, \mathrm{d}r \\ &+ \sigma_v \int_0^s K_n(s-r) \sqrt{v_n(t+r)}\, \mathrm{d}W_v(t+r). \end{aligned} \tag{44}$$

The continuation property of $\mathcal{G}_{K_n}$ therefore implies $g^{(n)}_{t,\boldsymbol{v}_n(t)} \in \mathcal{G}_{K_n}$ almost surely. Hence $\boldsymbol{v}_n(t) \in \mathcal{V}_n(t)$ for every t. The parameter values in Table 1 satisfy all the stated sign restrictions.

Assumption 1 (verification integrability). The initial wealth histories have finite fourth moments. Every feedback profile and each fixed bounded spike perturbation to which the verification theorem is applied have a pathwise unique delayed wealth solution and satisfy

$$\sup_{\pi} \mathbb{E}\left[\sup_{0 \leq s \leq T} \left(|\bar{Z}_{1n}(s)|^4 + |\bar{Z}_{2n}(s)|^4 \right) \right] < \infty, \tag{45}$$

where the supremum is over the feedback profile under verification and the indicated spike profiles. Together with (38), this condition is sufficient for all stopped Itô, domination, and uniform-integrability steps below. The explicit candidate and its bounded spike perturbations are verified in Proposition 1. We require nonnegativity of the aggregate variance, not positivity of individual factors, and do not assume strict positivity.

Let

$$\mathcal{X}_n = \{(t, \bar{z}_1, \bar{z}_2, \boldsymbol{\nu}) : t \in [0, T),\ (\bar{z}_1, \bar{z}_2) \in \mathbb{R}^2,\ \boldsymbol{\nu} \in \mathcal{V}_n(t)\}. \tag{46}$$

An admissible finite-factor feedback is a Borel map $\varphi_{kn} : \mathcal{X}_n \to \mathbb{U}_k$ that is locally Lipschitz on the interior of the viable set, has at most linear growth in its investment component, preserves Assumption 1, and satisfies (45). The associated feedback process is

$$\pi_{kn}(t) = \varphi_{kn}(t, \bar{Z}_{1n}(t), \bar{Z}_{2n}(t), \boldsymbol{\nu}_n(t)). \tag{47}$$

The joint wealth state is necessary for general feedbacks because the rival's action may depend on its own relative wealth. The explicit candidate derived below is deterministic and therefore extends to the whole joint state by ignoring the wealth and factor coordinates. The class of such feedbacks is Π_{kn}. Under (26)–(28), memory-adjusted relative wealth satisfies

$$\begin{aligned} \mathrm{d}\bar{Z}_{kn}(t) = {} & \Big[\bar{r}\bar{Z}_{kn}(t) + (\theta_k - \kappa_k\theta_j) + \eta_k a_{kn}(t) - \kappa_k \eta_j a_{jn}(t) \\ & \quad + m(b_{kn}(t) - \kappa_k b_{jn}(t))\nu_n(t, \boldsymbol{\nu}_n(t))\Big]\,\mathrm{d}t \\ & + \sigma_k a_{kn}(t)\,\mathrm{d}B_k(t) - \kappa_k \sigma_j a_{jn}(t)\,\mathrm{d}B_j(t) \\ & + (b_{kn}(t) - \kappa_k b_{jn}(t))\sqrt{\nu_n(t, \boldsymbol{\nu}_n(t))}\,\mathrm{d}W_s(t). \end{aligned} \tag{48}$$

The corresponding objective is

$$\begin{aligned} J_{kn}^{(\pi_{kn}, \pi_{jn}^*)}(t, \bar{z}_1, \bar{z}_2, \boldsymbol{\nu}) := {} & \mathbb{E}_{t,\bar{z}_1,\bar{z}_2,\boldsymbol{\nu}}\Big[\bar{Z}_{kn}^{(\pi_{kn}, \pi_{jn}^*)}(T)\Big] \\ & - \frac{\gamma_k}{2}\mathrm{Var}_{t,\bar{z}_1,\bar{z}_2,\boldsymbol{\nu}}\Big[\bar{Z}_{kn}^{(\pi_{kn}, \pi_{jn}^*)}(T)\Big]. \end{aligned} \tag{49}$$

The approximating game uses the same local action deviations as the rough problem. For a bounded $u_k \in \mathbb{U}_k$, define

$$\pi_{kn}^{t,\epsilon;u_k}(s) := \begin{cases} u_k, & t \le s < t + \epsilon, \\ \pi_{kn}^*(s), & t + \epsilon \le s \le T. \end{cases} \tag{50}$$

The pair (π_{1n}^*, π_{2n}^*) is an equilibrium if, for $k \neq j$, every bounded $u_k \in \mathbb{U}_k$, and every $(t, \bar{z}_1, \bar{z}_2, \boldsymbol{\nu}) \in \mathcal{X}_n$,

$$\liminf_{\epsilon \downarrow 0} \frac{J_{kn}^{(\pi_{kn}^*, \pi_{jn}^*)}(t, \bar{z}_1, \bar{z}_2, \boldsymbol{\nu}) - J_{kn}^{(\pi_{kn}^{t,\epsilon;u_k}, \pi_{jn}^*)}(t, \bar{z}_1, \bar{z}_2, \boldsymbol{\nu})}{\epsilon} \ge 0. \tag{51}$$

The two branches in (50) have distinct roles: The first is the local deviation, and the second is the candidate equilibrium continuation.

Kernel convergence alone does not preserve a time-consistent equilibrium. For a fixed $R < \infty$, let $\mathbb{U}_{k,R} = [0, 1] \times [-R, R]$. Define the one-step gain from the same action $u_k \in \mathbb{U}_{k,R}$ in both games by

$$\mathfrak{D}_k(\pi; u_k) := \limsup_{\epsilon \downarrow 0} \frac{J_k^{(\pi_k^{t,\epsilon;u_k}, \pi_j)} - J_k^{(\pi_k, \pi_j)}}{\epsilon}, \tag{52}$$

and define $\mathfrak{D}_{kn}$ analogously. For a finite-factor feedback φ_n, its lift to the rough filtration is obtained by evaluating φ_n at the exponential coordinates

$$v_{n,i}^{\uparrow}(t) = \int_0^t e^{-\gamma_{n,i}(t-s)}\Big[-\kappa v(s)\,\mathrm{d}s + \sigma_v\sqrt{v(s)}\,\mathrm{d}W_v(s)\Big], \qquad i = 1, \ldots, n. \tag{53}$$

The deterministic term g_n contains the corresponding v_0 and $\kappa\omega$ contributions. Initial states are paired by starting both models from the same wealth history and mapping the rough-volatility history to (53). We assume that the resulting coordinates lie in $\mathcal{V}_n(t)$. If a finite-factor feedback is defined only on the reachable set, its lift uses a measurable admissible extension to $\mathcal{X}_n$; the explicit feedbacks below already have such an extension because they are functions of time only.

Theorem 1. *Fix $R < \infty$. Let $\pi_n^* = (\pi_{1n}^*, \pi_{2n}^*)$ be equilibrium profiles of the n-factor games and let $\pi_n^{*,\uparrow}$ denote their admissible lifts through* (53)*. Assume that $K_n \to K$ in $L^2(0,T)$, the paired controlled states converge in L^2 under this lift, the terminal relative wealths are uniformly square integrable, and, on every compact set of paired initial states,*

$$\sup_{k\in\{1,2\}} \sup_{u_k\in\mathbb{U}_{k,R}} \left|\mathfrak{D}_k(\pi_n^{*,\uparrow}; u_k) - \mathfrak{D}_{kn}(\pi_n^*; u_k)\right| \longrightarrow 0. \tag{54}$$

Then, for every $\varepsilon > 0$, there exists N such that, for $n \geq N$,

$$\sup_{u_k\in\mathbb{U}_{k,R}} \mathfrak{D}_k(\pi_n^{*,\uparrow}; u_k) \leq \varepsilon, \qquad k = 1, 2. \tag{55}$$

Thus $\pi_n^{*,\uparrow}$ is an ε-equilibrium against constant spike actions in the fixed compact set $\mathbb{U}_{k,R}$. Uniform convergence of local-deviation gains yields this ε-equilibrium property on the fixed compact action set. The result is deliberately conditional: It does not derive the local-gain convergence in (54) *from kernel convergence alone. Extending the result to the unbounded investment set requires an additional uniform coercivity result that places all maximizing deviations in one common compact set.*

Proof. For fixed R, set

$$\delta_n(R) := \sup_{k\in\{1,2\}} \sup_{u_k\in\mathbb{U}_{k,R}} \left|\mathfrak{D}_k(\pi_n^{*,\uparrow}; u_k) - \mathfrak{D}_{kn}(\pi_n^*; u_k)\right|. \tag{56}$$

Assumption (54) is precisely $\delta_n(R) \to 0$. Given $\varepsilon > 0$, choose N such that

$$n \geq N \quad \Longrightarrow \quad \delta_n(R) \leq \varepsilon. \tag{57}$$

For $n \geq N$, $k \in \{1, 2\}$, and $u_k \in \mathbb{U}_{k,R}$, the finite-factor equilibrium property gives

$$\mathfrak{D}_{kn}(\pi_n^*; u_k) \leq 0. \tag{58}$$

Consequently,

$$\begin{aligned} \mathfrak{D}_k(\pi_n^{*,\uparrow}; u_k) &= \mathfrak{D}_{kn}(\pi_n^*; u_k) + \left[\mathfrak{D}_k(\pi_n^{*,\uparrow}; u_k) - \mathfrak{D}_{kn}(\pi_n^*; u_k)\right] \\ &\leq \left|\mathfrak{D}_k(\pi_n^{*,\uparrow}; u_k) - \mathfrak{D}_{kn}(\pi_n^*; u_k)\right| \leq \delta_n(R) \leq \varepsilon. \end{aligned} \tag{59}$$

Taking the supremum over $u_k \in \mathbb{U}_{k,R}$ proves (55). The state convergence and uniform square-integrability assumptions ensure that the two local gains appearing in $\delta_n(R)$ are well defined; uniform local-deviation-gain convergence then yields the stated conclusion.

4. Nash equilibrium

This section verifies the local Nash equilibrium of the finite-dimensional approximating game through its Markovian state representation. For general feedbacks the Markov state is

$$(\bar{Z}_{1n}, \bar{Z}_{2n}, \boldsymbol{v}_n) \in \mathcal{X}_n. \tag{60}$$

The full generator includes the second wealth coordinate and its covariations. The affine candidate and the test functions used below do not depend on the rival's wealth coordinate. For such a test function $\phi(t, \bar{z}_k, \boldsymbol{\nu}) \in C^{1,2}$, with insurer j's feedback fixed, the nonzero part of the full generator is displayed in (62). The verification theorem applies to candidate functions of the form

$$\phi(t, \bar{z}_1, \bar{z}_2, \boldsymbol{\nu}) = \widetilde{\phi}(t, \bar{z}_k, \boldsymbol{\nu}). \tag{61}$$

The deterministic affine candidate has this form and satisfies the reduced HJB equation.

$$\begin{aligned}
\mathcal{A}^{(\pi_{kn}, \pi^*_{jn})}\phi = \phi_t &+ \sum_{i=1}^{n}(-\gamma_{n,i}\nu_i - \kappa\nu_n)\phi_{\nu_i} \\
&+ \Big[\bar{r}\bar{z} + (\theta_k - \kappa_k\theta_j) + \eta_k a_k - \kappa_k\eta_j a^*_{jn} + m\nu_n(b_k - \kappa_k b^*_{jn})\Big]\phi_{\bar{z}} \\
&+ \frac{1}{2}\Big[\sigma_k^2 a_k^2 + \kappa_k^2\sigma_j^2(a^*_{jn})^2 - 2\kappa_k\rho_{12}\sigma_k\sigma_j a_k a^*_{jn} + \nu_n(b_k - \kappa_k b^*_{jn})^2\Big]\phi_{\bar{z}\bar{z}} \\
&+ \frac{1}{2}\sigma_v^2\nu_n\sum_{i=1}^{n}\sum_{\ell=1}^{n}\phi_{\nu_i\nu_\ell} + \sigma_v\rho_{\mathrm{sv}}\nu_n(b_k - \kappa_k b^*_{jn})\sum_{i=1}^{n}\phi_{\bar{z}\nu_i},
\end{aligned} \tag{62}$$

where $\bar{z} = \bar{z}_k$, while the opponent's feedback is evaluated at the full state $(t, \bar{z}_1, \bar{z}_2, \boldsymbol{\nu})$. The double sum is required because every factor in (28) is driven by the same Brownian motion W_v. Define the carré-du-champ operator

$$\Gamma^{(\pi_{kn}, \pi^*_{jn})}\phi := \mathcal{A}^{(\pi_{kn}, \pi^*_{jn})}(\phi^2) - 2\phi\,\mathcal{A}^{(\pi_{kn}, \pi^*_{jn})}\phi. \tag{63}$$

When only the current action is varied, we write $\mathcal{A}^{(u_k, \pi^*_{jn})}$ and $\Gamma^{(u_k, \pi^*_{jn})}$, with $u_k = (a_k, b_k) \in \mathbb{U}_k$.

Theorem 2. *Assume that the controlled joint-state equation has a unique non-explosive solution for every admissible feedback and that* (45) *holds. Suppose that V_{kn} and g_{kn} admit $C^{1,2}$ extensions to $[0, T) \times \mathbb{R}^{n+2}$, and have growth of degree at most two in the wealth variables and at most one in the factor coordinates. For $R \geq 1$, define*

$$\tau_R := \inf\Big\{s \in [t, T] : |\bar{Z}_{1n}(s)| + |\bar{Z}_{2n}(s)| + \|\boldsymbol{\nu}_n(s)\| \geq R\Big\} \wedge T. \tag{64}$$

Assume that $\tau_R \uparrow T$ almost surely, that the stopped stochastic integrals are true martingales, and that

$$\{V_{kn}(\tau_R, X_{\tau_R}),\ g_{kn}(\tau_R, X_{\tau_R}),\ g^2_{kn}(\tau_R, X_{\tau_R})\}_{R\geq 1} \tag{65}$$

is uniformly integrable. Assume also that the generator expressions are continuous in the state, locally uniformly for u_k in compact subsets of $\mathbb{U}_k$, and are dominated by an integrable polynomial envelope under bounded spike actions. Finally, suppose that the feedback profile (π^*_{1n}, π^*_{2n}) is admissible. For each $k \neq j$, suppose that the candidate functions are independent of the rival wealth coordinate,

$$V_{kn}(t, \bar{z}_1, \bar{z}_2, \boldsymbol{\nu}) = V_{kn}(t, \bar{z}_k, \boldsymbol{\nu}), \qquad g_{kn}(t, \bar{z}_1, \bar{z}_2, \boldsymbol{\nu}) = g_{kn}(t, \bar{z}_k, \boldsymbol{\nu}). \tag{66}$$

$$\sup_{u_k \in \mathbb{U}_k}\Big\{\mathcal{A}^{(u_k, \pi^*_{jn})}V_{kn} - \frac{\gamma_k}{2}\mathcal{A}^{(u_k, \pi^*_{jn})}(g^2_{kn}) + \gamma_k g_{kn}\mathcal{A}^{(u_k, \pi^*_{jn})}g_{kn}\Big\} = 0, \tag{67}$$

$$V_{kn}(T, \bar{z}_1, \bar{z}_2, \boldsymbol{\nu}) = \bar{z}_k, \tag{68}$$

$$\mathcal{A}^{(\pi^*_{kn},\pi^*_{jn})} g_{kn} = 0, \tag{69}$$

$$g_{kn}(T, \bar{z}_1, \bar{z}_2, \boldsymbol{\nu}) = \bar{z}_k, \tag{70}$$

and

$$\pi^*_{kn} \in \arg\max_{u_k \in \mathbb{U}_k} \Big\{ \mathcal{A}^{(u_k,\pi^*_{jn})} V_{kn} - \frac{\gamma_k}{2} \mathcal{A}^{(u_k,\pi^*_{jn})}(g^2_{kn}) + \gamma_k g_{kn} \mathcal{A}^{(u_k,\pi^*_{jn})} g_{kn} \Big\}. \tag{71}$$

All these generator identities are required to hold at every viable state, including states with $\nu_n = 0$. Then

$$g_{kn}(t, \bar{z}_1, \bar{z}_2, \boldsymbol{\nu}) = \mathbb{E}_{t,\bar{z}_1,\bar{z}_2,\boldsymbol{\nu}} \Big[\bar{Z}^{(\pi^*_{kn},\pi^*_{jn})}_{kn}(T) \Big], \qquad V_{kn} = J^{(\pi^*_{kn},\pi^*_{jn})}_{kn}, \tag{72}$$

and (π^*_{1n}, π^*_{2n}) is a time-consistent Nash equilibrium in the sense of (50).

Proof. Fix k and keep π^*_{jn} fixed. Write $X_s = (\bar{Z}_{1n}(s), \bar{Z}_{2n}(s), \boldsymbol{\nu}_n(s))$ and use the stopping times τ_R defined in the theorem. Non-explosion gives $\tau_R \uparrow T$ almost surely. The $C^{1,2}$ extensions permit Itô's formula along the whole viable path, including any visits to $\nu_n = 0$; the generator identities remain valid there by hypothesis. Under the candidate profile, Itô's formula and (69) give

$$g_{kn}(s \wedge \tau_R, X_{s\wedge\tau_R}) = g_{kn}(t, X_t) + M_{s\wedge\tau_R}, \tag{73}$$

where

$$M_{s\wedge\tau_R} = \int_t^{s\wedge\tau_R} \mathrm{d}M^g_r, \qquad \mathrm{d}\langle M^g \rangle_r = \Gamma^{(\pi^*_{kn},\pi^*_{jn})} g_{kn}(r, X_r)\, \mathrm{d}r. \tag{74}$$

The second identity follows from the definition of the carré-du-champ operator. In particular,

$$\mathbb{E}_t[M_{s\wedge\tau_R}] = 0, \qquad \mathbb{E}_t[M^2_{s\wedge\tau_R}] = \mathbb{E}_t \int_t^{s\wedge\tau_R} \Gamma^{(\pi^*_{kn},\pi^*_{jn})} g_{kn}(r, X_r)\, \mathrm{d}r. \tag{75}$$

Letting first $s \uparrow T$ and then $R \uparrow \infty$, the fourth-moment bound in (45), polynomial growth of g_{kn}, and uniform integrability give

$$g_{kn}(t, X_t) = \mathbb{E}_t[\bar{Z}_{kn}(T)]. \tag{76}$$

Moreover,

$$\mathrm{Var}_t[\bar{Z}_{kn}(T)] = \mathbb{E}_t \int_t^T \Gamma^{(\pi^*_{kn},\pi^*_{jn})} g_{kn}(s, X_s)\, \mathrm{d}s. \tag{77}$$

Indeed, $g_{kn}(T, X_T) = \bar{Z}_{kn}(T)$ by (70); hence

$$\bar{Z}_{kn}(T) - \mathbb{E}_t[\bar{Z}_{kn}(T)] = M^g_T - M^g_t. \tag{78}$$

Conditional Itô isometry then gives the displayed variance identity.

For $u_k \in \mathbb{U}_k$, define

$$\mathcal{H}_k(u_k) := \mathcal{A}^{(u_k,\pi^*_{jn})} V_{kn} - \frac{\gamma_k}{2} \mathcal{A}^{(u_k,\pi^*_{jn})}(g^2_{kn}) + \gamma_k g_{kn} \mathcal{A}^{(u_k,\pi^*_{jn})} g_{kn}. \tag{79}$$

The identity

$$\mathcal{A}^{(u_k,\pi^*_{jn})}(g^2_{kn}) = 2 g_{kn} \mathcal{A}^{(u_k,\pi^*_{jn})} g_{kn} + \Gamma^{(u_k,\pi^*_{jn})} g_{kn} \tag{80}$$

shows that, at the candidate feedback,

$$\mathcal{H}_k(\pi_{kn}^*) = \mathcal{A}^{(\pi_{kn}^*,\pi_{jn}^*)}V_{kn} - \frac{\gamma_k}{2}\Gamma^{(\pi_{kn}^*,\pi_{jn}^*)}g_{kn}. \tag{81}$$

Since (67) and (71) give $\mathcal{H}_k(\pi_{kn}^*) = 0$, while (69) gives $\mathcal{A}^{(\pi_{kn}^*,\pi_{jn}^*)}g_{kn} = 0$, we obtain

$$\mathcal{A}^{(\pi_{kn}^*,\pi_{jn}^*)}V_{kn} = \frac{\gamma_k}{2}\Gamma^{(\pi_{kn}^*,\pi_{jn}^*)}g_{kn}. \tag{82}$$

Applying Itô's formula to $V_{kn}(s, X_s)$, then taking conditional expectations and passing through the same localization limit, gives

$$\mathbb{E}_t[V_{kn}(T, X_T)] - V_{kn}(t, X_t) = \frac{\gamma_k}{2}\mathbb{E}_t\int_t^T \Gamma^{(\pi_{kn}^*,\pi_{jn}^*)}g_{kn}(s, X_s)\,\mathrm{d}s. \tag{83}$$

Using (68), (70), and the preceding variance identity therefore gives

$$V_{kn}(t, X_t) = \mathbb{E}_t[\bar{Z}_{kn}(T)] - \frac{\gamma_k}{2}\mathrm{Var}_t[\bar{Z}_{kn}(T)]. \tag{84}$$

Thus V_{kn} is the equilibrium payoff generated by the candidate profile.

It remains to verify the local deviation condition. Let insurer k use a bounded constant action $u_k \in \mathbb{U}_k$ on $[t, t+\epsilon)$ and return to π_{kn}^* thereafter. Conditional on $X_{t+\epsilon}^\epsilon$, the continuation mean and continuation payoff are $g_{kn}(t+\epsilon, X_{t+\epsilon}^\epsilon)$ and $V_{kn}(t+\epsilon, X_{t+\epsilon}^\epsilon)$. The conditional variance decomposition gives

$$\begin{aligned} J_{kn}^{(\pi_{kn}^{t,\epsilon;u_k},\pi_{jn}^*)}(t, X_t) = \mathbb{E}_t\big[V_{kn}(t+\epsilon, X_{t+\epsilon}^\epsilon)\big] \\ - \frac{\gamma_k}{2}\mathrm{Var}_t\big[g_{kn}(t+\epsilon, X_{t+\epsilon}^\epsilon)\big]. \end{aligned} \tag{85}$$

Indeed, the conditional continuation identities imply

$$\begin{aligned} \mathbb{E}_t[\bar{Z}_{kn}(T)] &= \mathbb{E}_t\big[g_{kn}(t+\epsilon, X_{t+\epsilon}^\epsilon)\big], \\ \mathrm{Var}_t[\bar{Z}_{kn}(T)] &= \mathbb{E}_t\Big[\mathrm{Var}_{t+\epsilon}\Big(\bar{Z}_{kn}(T)\Big)\Big] + \mathrm{Var}_t\big[g_{kn}(t+\epsilon, X_{t+\epsilon}^\epsilon)\big]. \end{aligned} \tag{86}$$

Substitution of the definition of V_{kn} at time $t+\epsilon$ gives equation (85). For the localized process, Itô's formula and the polynomial envelope give, uniformly for u_k in a fixed compact action set,

$$\begin{aligned} \mathbb{E}_t[V_{kn}(t+\epsilon, X_{t+\epsilon}^\epsilon)] &= V_{kn}(t, X_t) + \epsilon\mathcal{A}^{(u_k,\pi_{jn}^*)}V_{kn}(t, X_t) + o(\epsilon), \\ \mathbb{E}_t[g_{kn}(t+\epsilon, X_{t+\epsilon}^\epsilon)] &= g_{kn}(t, X_t) + \epsilon\mathcal{A}^{(u_k,\pi_{jn}^*)}g_{kn}(t, X_t) + o(\epsilon), \\ \mathbb{E}_t[g_{kn}^2(t+\epsilon, X_{t+\epsilon}^\epsilon)] &= g_{kn}^2(t, X_t) + \epsilon\mathcal{A}^{(u_k,\pi_{jn}^*)}(g_{kn}^2)(t, X_t) + o(\epsilon). \end{aligned} \tag{87}$$

It follows that

$$\mathrm{Var}_t[g_{kn}(t+\epsilon, X_{t+\epsilon}^\epsilon)] = \epsilon\Big[\mathcal{A}^{(u_k,\pi_{jn}^*)}(g_{kn}^2) - 2g_{kn}\mathcal{A}^{(u_k,\pi_{jn}^*)}g_{kn}\Big]_{(t,X_t)} + o(\epsilon). \tag{88}$$

Combining equations (87) and (88) gives

$$\begin{aligned} J_{kn}^{(\pi_{kn}^{t,\epsilon;u_k},\pi_{jn}^*)} - V_{kn} = \epsilon\Big[\mathcal{A}^{(u_k,\pi_{jn}^*)}V_{kn} - \frac{\gamma_k}{2}\mathcal{A}^{(u_k,\pi_{jn}^*)}(g_{kn}^2) \\ + \gamma_k g_{kn}\mathcal{A}^{(u_k,\pi_{jn}^*)}g_{kn}\Big]_{(t,X_t)} + o(\epsilon). \end{aligned} \tag{89}$$

The $o(\epsilon)$ remainder is uniform for u_k in each compact action set. It follows by applying the integrable polynomial envelope to the localized generator difference, using (45), and then removing localization by uniform integrability. The bracket equals $\mathcal{H}_k(u_k)$, and therefore $\mathcal{H}_k(u_k) \le 0$ by (67); it equals zero when $u_k = \pi^*_{kn}(t, X_t)$ by (71). Consequently,

$$\liminf_{\epsilon \downarrow 0} \frac{V_{kn}(t, X_t) - J_{kn}^{(\pi_{kn}^{t,\epsilon;u_k}, \pi^*_{jn})}(t, X_t)}{\epsilon} \ge 0. \tag{90}$$

This is (50). Applying the same argument to $k = 1$ and $k = 2$ proves the Nash equilibrium assertion.

We next derive the closed-form equilibrium strategies and value functions. For compactness, z denotes the transformed state $\bar{z}$. We retain the symbol $\bar{r}$ for the effective accumulation rate to distinguish it from the risk-free rate r_f.

By Theorem 2, the first-order conditions characterize the equilibrium strategy. Differentiating (71) with respect to π_k, we obtain

$$a^*_k(t) = -\frac{\eta_k V_{k,z}}{\sigma_k^2(V_{k,zz} - \gamma_k(g_{k,z})^2)} + \kappa_k \rho_{12} \frac{\sigma_j}{\sigma_k} a^*_j(t), \tag{91}$$

$$b^*_k(t) = -\frac{m V_{k,z} + \sigma_v \rho_{\mathrm{sv}} \sum_{i=1}^n (V_{k,zv_i} - \gamma_k g_{k,z} g_{k,v_i})}{V_{k,zz} - \gamma_k (g_{k,z})^2} + \kappa_k b^*_j(t). \tag{92}$$

Put $D_k := V_{k,zz} - \gamma_k(g_{k,z})^2 < 0$ and $q^*_k := b^*_k - \kappa_k b^*_j$. Substituting (91)–(92) into (67) gives the optimized equation

$$\begin{aligned} 0 = {} & V_{k,t} + [\bar{r}z + (\theta_k - \kappa_k \theta_j) - \kappa_k \eta_j a^*_j(t)] V_{k,z} \\ & + \sum_{i=1}^n (-\gamma_{n,i} v_i - \kappa \nu_n) V_{k,v_i} + \frac{\sigma_v^2 \nu_n}{2} \sum_{i=1}^n \sum_{\ell=1}^n (V_{k,v_i v_\ell} - \gamma_k g_{k,v_i} g_{k,v_\ell}) \\ & + \frac{D_k}{2} \kappa_k^2 \sigma_j^2 (a^*_j)^2 - \frac{[\eta_k V_{k,z} - D_k \kappa_k \rho_{12} \sigma_k \sigma_j a^*_j]^2}{2 D_k \sigma_k^2} \\ & - \frac{\nu_n}{2 D_k} \left[m V_{k,z} + \sigma_v \rho_{\mathrm{sv}} \sum_{i=1}^n (V_{k,zv_i} - \gamma_k g_{k,z} g_{k,v_i}) \right]^2 . \end{aligned} \tag{93}$$

Under the candidate profile, the conditional-mean equation (69) is

$$\begin{aligned} 0 = {} & g_{k,t} + [\bar{r}z + (\theta_k - \kappa_k \theta_j) + \eta_k a^*_k - \kappa_k \eta_j a^*_j + m \nu_n q^*_k] g_{k,z} \\ & + \sum_{i=1}^n (-\gamma_{n,i} v_i - \kappa \nu_n) g_{k,v_i} \\ & + \frac{1}{2} \Big[\sigma_k^2 (a^*_k)^2 + \kappa_k^2 \sigma_j^2 (a^*_j)^2 - 2 \kappa_k \rho_{12} \sigma_k \sigma_j a^*_k a^*_j + \nu_n (q^*_k)^2 \Big] g_{k,zz} \\ & + \frac{\sigma_v^2 \nu_n}{2} \sum_{i=1}^n \sum_{\ell=1}^n g_{k,v_i v_\ell} + \sigma_v \rho_{\mathrm{sv}} \nu_n q^*_k \sum_{i=1}^n g_{k,zv_i}. \end{aligned} \tag{94}$$

To solve (93) and (94), we use the affine ansatz

$$V_k(t,z,v) = A(t)z + \sum_{i=1}^{n} \frac{B_i(t)}{\gamma_k} v_i + \frac{C_k(t)}{\gamma_k}, \qquad A(T) = 1,\ B_i(T) = C_k(T) = 0, \tag{95}$$

$$g_k(t,z,\boldsymbol{v}) = \hat{A}(t)z + \sum_{i=1}^{n} \frac{\hat{B}_i(t)}{\gamma_k} v_i + \frac{\hat{C}_k(t)}{\gamma_k}, \qquad \hat{A}(T) = 1,\ \hat{B}_i(T) = \hat{C}_k(T) = 0. \tag{96}$$

The partial derivatives are

$$V_{k,t}(t,z,v) = A'(t)z + \sum_{i=1}^{n} \frac{B_i'(t)}{\gamma_k} v_i + \frac{C_k'(t)}{\gamma_k}, \tag{97}$$

$$g_{k,t}(t,z,\boldsymbol{v}) = \hat{A}'(t)z + \sum_{i=1}^{n} \frac{\hat{B}_i'(t)}{\gamma_k} v_i + \frac{\hat{C}_k'(t)}{\gamma_k}. \tag{98}$$

Substituting these derivatives into (91) and (92) yields

$$a_k^*(t) = \frac{\eta_k e^{-\bar{r}(T-t)}}{\gamma_k \sigma_k^2} + \kappa_k \rho_{12} \frac{\sigma_j}{\sigma_k} a_j^*(t), \tag{99}$$

$$b_k^*(t) = \frac{mA}{\gamma_k \hat{A}^2} - \frac{\sigma_v \rho_{\mathrm{sv}}}{\gamma_k \hat{A}} \sum_{i=1}^{n} \hat{B}_i + \kappa_k b_j^*(t). \tag{100}$$

The factors in (99)–(100) follow directly from $-V_{k,z}/(V_{k,zz} - \gamma_k g_{k,z}^2) = A/(\gamma_k \hat{A}^2) = e^{-\bar{r}(T-t)}/\gamma_k$ and $\gamma_k g_{k,z} g_{k,v_i} = \hat{A}\hat{B}_i$. Hence the reinsurance diffusion contributes $\sigma_k^2 a_k^2$, while the volatility-hedging term is $-\sigma_v \rho_{\mathrm{sv}} e^{-\bar{r}(T-t)} \sum_i \hat{B}_i(t)/\gamma_k$. Equations (99) and (100) show two distinct strategic channels. Retention reacts to the competitor only through $\kappa_k \rho_{12} \sigma_j/\sigma_k$; hence this cross-response disappears when $\rho_{12} = 0$. Investment reacts through κ_k even when claim risks are uncorrelated. Without relative-performance concern, the two controls reduce to their direct mean–variance and volatility-hedging components. Reinsurance and stock investment are parallel control channels in the model: Their respective diffusion terms determine the two controls, and the constraint structure has no capital-transfer mechanism between them.

We next solve the coefficient equations. The common Brownian driver in (28) couples the factor coefficients; consequently, they cannot be solved as n unrelated scalar ordinary differential equations (ODEs). Let

$$\boldsymbol{c} = (c_{n,1}, \ldots, c_{n,n})^\top, \qquad D_n = \mathrm{diag}(\gamma_{n,1}, \ldots, \gamma_{n,n}), \qquad \mathbf{1} = (1, \ldots, 1)^\top. \tag{101}$$

The coefficients of z in (93)–(94) give

$$A(t) = \hat{A}(t) = e^{\bar{r}(T-t)}. \tag{102}$$

Write $\widehat{\boldsymbol{B}} = (\hat{B}_1, \ldots, \hat{B}_n)^\top$, $S_{\hat{B}} = \mathbf{1}^\top \widehat{\boldsymbol{B}}$, and

$$M_g = D_n + (\kappa + m\sigma_v \rho_{\mathrm{sv}}) \boldsymbol{c} \mathbf{1}^\top. \tag{103}$$

The coefficients of $(v_1, \dots, v_n)$ in the martingale equation (69) satisfy the coupled terminal-value problem

$$\widehat{\boldsymbol{B}}'(t) = M_g \widehat{\boldsymbol{B}}(t) - m^2 \boldsymbol{c}, \qquad \widehat{\boldsymbol{B}}(T) = \mathbf{0}. \tag{104}$$

Hence

$$\widehat{\boldsymbol{B}}(t) = m^2 \int_t^T e^{-M_g(s-t)} \boldsymbol{c}\, \mathrm{d}s = m^2 M_g^{-1}(I - e^{-M_g(T-t)})\boldsymbol{c}, \tag{105}$$

with the integral representation applying also when M_g is singular. This matrix has two rank-one sources. The term $\kappa \boldsymbol{c}\mathbf{1}^\top$ comes from the drift of the aggregate variance, while $m\sigma_v \rho_{\mathrm{sv}} \boldsymbol{c}\mathbf{1}^\top$ comes from the stock–variance hedging feedback. These drift and feedback couplings should not be conflated with cross-factor second-order covariations. The latter arise from the common Brownian driver and appear explicitly in the double sum in (62) and in the squared sums entering $R(t)$.

For the value function, let $\boldsymbol{B} = (B_1, \dots, B_n)^\top$, $S_B = \mathbf{1}^\top \boldsymbol{B}$, and

$$R(t) = \frac{1}{2}\left[(m - \sigma_v \rho_{\mathrm{sv}} S_{\hat{B}}(t))^2 - \sigma_v^2 S_{\hat{B}}^2(t)\right]. \tag{106}$$

Then the factor coefficients solve

$$\begin{aligned} \boldsymbol{B}'(t) &= (D_n + \kappa \boldsymbol{c}\mathbf{1}^\top)\boldsymbol{B}(t) - \boldsymbol{c}R(t), \qquad \boldsymbol{B}(T) = \mathbf{0}, \\ \boldsymbol{B}(t) &= \int_t^T e^{-(D_n + \kappa \boldsymbol{c}\mathbf{1}^\top)(s-t)} \boldsymbol{c} R(s)\, \mathrm{d}s. \end{aligned} \tag{107}$$

Finally, define

$$\begin{aligned} C_k(t) :=\ & \gamma_k(\theta_k - \kappa_k \theta_j)A(t) - \kappa g_n(t) S_B(t) + \gamma_k A(t)[\eta_k a_k^*(t) - \kappa_k \eta_j a_j^*(t)] \\ & - \frac{\gamma_k^2}{2}\hat{A}^2(t)\Big[\sigma_k^2 (a_k^*(t))^2 + \kappa_k^2 \sigma_j^2 (a_j^*(t))^2 - 2\kappa_k \rho_{12} \sigma_k \sigma_j a_k^*(t) a_j^*(t)\Big] + g_n(t) R(t), \end{aligned} \tag{108}$$

$$\begin{aligned} \widehat{C}_k(t) :=\ & \gamma_k[\theta_k - \kappa_k \theta_j + \eta_k a_k^*(t) - \kappa_k \eta_j a_j^*(t)]\hat{A}(t) - \kappa g_n(t) S_{\hat{B}}(t) \\ & + m g_n(t)[m - \sigma_v \rho_{\mathrm{sv}} S_{\hat{B}}(t)]. \end{aligned} \tag{109}$$

The remaining coefficients are

$$C_k(t) = \int_t^T C_k(s)\, \mathrm{d}s, \qquad \hat{C}_k(t) = \int_t^T \widehat{C}_k(s)\, \mathrm{d}s. \tag{110}$$

Substitution in (93)–(94) verifies these coefficient equations directly. In particular, (105) replaces the scalar-factor formula and retains all common-driver cross terms.

The form (108) is written directly in terms of the retention controls and therefore remains valid when a projected retention constraint binds. The shorter expression obtained by substituting an interior first-order condition must not be used at the boundary.

Proposition 1. *The coefficient $\widehat{\boldsymbol{B}}$ is continuous and bounded on $[0, T]$ because it is an integral of a matrix exponential over a finite interval. Consequently, the explicit investment controls below are deterministic, continuous, and bounded. The projected retention controls take values in $[0, 1]$. Fix $t_0 \in [0, T]$ and $\boldsymbol{v}^0 \in \mathcal{V}_n(t_0)$. For every initial wealth history on $[t_0 - h, t_0]$ with finite fourth moment,*

$$\mathbb{E}_{t_0} \int_{t_0}^T |b_k^*(s)|^4\, \mathrm{d}s \le T \sup_{s \le T} |b_k^*(s)|^4 < \infty. \tag{111}$$

For every fixed bounded spike perturbation, the resulting control profile is admissible and satisfies (45). *The affine candidates also satisfy the uniform-integrability requirements of Theorem 2.*

Proof. Fix a bounded spike set $\mathbb{U}_{k,R}$ and let

$$\bar{b}_R := \max_{\ell\in\{1,2\}} \sup_{0\le s\le T} |b^*_\ell(s)| \vee R < \infty. \tag{112}$$

Fix $t_0 \in [0,T]$ and $\boldsymbol{\nu}^0 \in \mathcal{V}_n(t_0)$. The continuation property used in Lemma 1 yields a nonnegative factor solution started from $\boldsymbol{\nu}^0$. Define

$$F_s := \max_{1\le i\le n} \sup_{t_0\le u\le s} |\nu_{n,i}(u)|, \qquad t_0 \le s \le T. \tag{113}$$

Since g_n is bounded on $[0,T]$, (27) gives

$$0 \le \nu_n(s) \le C(1+F_s), \qquad t_0 \le s \le T. \tag{114}$$

Variation of constants in (28) from t_0 to s gives

$$\begin{aligned}\nu_{n,i}(s) = e^{-\gamma_{n,i}(s-t_0)}\nu^0_{n,i} - \kappa\int_{t_0}^{s} e^{-\gamma_{n,i}(s-u)}\nu_n(u)\,\mathrm{d}u \\ + \sigma_\nu\int_{t_0}^{s} e^{-\gamma_{n,i}(s-u)}\sqrt{\nu_n(u)}\,\mathrm{d}W_\nu(u).\end{aligned} \tag{115}$$

The Burkholder–Davis inequality, Cauchy–Schwarz inequality, and the preceding bound imply

$$\mathbb{E}_{t_0}[F_s^4] \le C\left(1 + \|\boldsymbol{\nu}^0\|^4 + \int_{t_0}^{s}\mathbb{E}_{t_0}[F_u^4]\,\mathrm{d}u\right). \tag{116}$$

Gronwall's inequality therefore yields

$$\sup_{t_0\le s\le T}\mathbb{E}_{t_0}[F_s^4] < \infty, \qquad \sup_{t_0\le s\le T}\mathbb{E}_{t_0}[\nu_n^4(s)] < \infty. \tag{117}$$

The candidate investment controls are bounded by the first assertion, while a spike investment is bounded by R and every retention lies in $[0,1]$. For the wealth processes generated by the candidate profile or by one such spike, set

$$D_s := \max_{\ell\in\{1,2\}} \sup_{t_0-h\le u\le s} |X_\ell(u)|. \tag{118}$$

Since $q_\delta\int_{-h}^{0} e^{\delta u}\,\mathrm{d}u = 1$, the delay variables satisfy

$$|M_\ell(s)| \le D_s, \qquad |N_\ell(s)| \le D_s, \qquad t_0 \le s \le T. \tag{119}$$

Writing the drift and the two diffusion coefficients in (10) as $\mathfrak{b}_\ell$, $\mathfrak{s}_{\ell,B}$, and $\mathfrak{s}_{\ell,W}$, respectively, the bounded-control property gives a constant $C_R < \infty$ such that

$$|\mathfrak{b}_\ell(s)| \le C_R(1 + D_s + \nu_n(s)), \qquad |\mathfrak{s}_{\ell,B}(s)|^2 + |\mathfrak{s}_{\ell,W}(s)|^2 \le C_R(1+\nu_n(s)). \tag{120}$$

The Burkholder–Davis–Gronwall estimates therefore yield

$$\mathbb{E}_{t_0}[D_s^4] \le C_R\left(1 + \mathbb{E}_{t_0}[D_{t_0}^4] + \int_{t_0}^{s} \mathbb{E}_{t_0}[\nu_n^4(u)]\,\mathrm{d}u + \int_{t_0}^{s} \mathbb{E}_{t_0}[D_u^4]\,\mathrm{d}u\right), \qquad t_0 \le s \le T. \tag{121}$$

The factor estimate above makes the variance integral finite. Gronwall's inequality consequently gives

$$\sup_{t_0\le s\le T} \mathbb{E}_{t_0}[D_s^4] < \infty, \tag{122}$$

which implies (45) because $|\bar{Z}_\ell| \le CD_T$. To establish pathwise uniqueness, let X and $\widetilde{X}$ be two solutions with the same initial history, factor path, Brownian motions, and candidate-or-spike control. Put

$$\Delta_\ell(s) := X_\ell(s) - \widetilde{X}_\ell(s), \qquad \Delta D_s := \max_{\ell\in\{1,2\}} \sup_{t_0-h\le u\le s} |\Delta_\ell(u)|. \tag{123}$$

The diffusion terms cancel in the difference of (11), and

$$\Delta_\ell(s) = \int_{t_0}^{s} \left[r_1\Delta_\ell(u) + \alpha\Delta M_\ell(u) + \beta\Delta N_\ell(u)\right]\mathrm{d}u. \tag{124}$$

The normalized kernels give

$$|\Delta M_\ell(u)| \le \Delta D_u, \qquad |\Delta N_\ell(u)| \le \Delta D_u, \tag{125}$$

and hence

$$\Delta D_s \le (|r_1| + |\alpha| + |\beta|)\int_{t_0}^{s} \Delta D_u\,\mathrm{d}u. \tag{126}$$

Because $\Delta D_{t_0} = 0$, Gronwall's inequality gives $\Delta D_s = 0$ for all $s \in [t_0, T]$. Thus the delayed wealth solution is pathwise unique.

The displayed affine forms of V_{kn} and g_{kn} and the two preceding conditional fourth-moment estimates imply

$$\sup_{\tau\in[t_0,T]} \mathbb{E}_{t_0}\left[|V_{kn}(\tau, X_\tau)|^2 + |g_{kn}(\tau, X_\tau)|^4\right] < \infty, \tag{127}$$

where the supremum is over the localization stopping times. Hence the stopped families of V_{kn}, g_{kn}, and g_{kn}^2 are uniformly integrable. This verifies the admissibility and integrability hypotheses required in Theorem 2.

Theorem 3. *Suppose that Assumption 1 holds and $\kappa_1\kappa_2 < 1$. Because $|\rho_{12}| \le 1$, this condition also implies $\kappa_1\kappa_2\rho_{12}^2 < 1$. Suppose that the retention candidates lie in* $(0, 1)$. *Then the n-factor game has an explicit time-consistent Nash equilibrium. Within the affine ansatz and the interior coupled best-response system, its coefficient solution is unique. Its best-response system separates the two correlation channels. The reinsurance equations contain the insurer–insurer claim-risk correlation ρ_{12}, whereas the investment equations contain the stock–variance correlation ρ_{sv}. Solving the investment system introduces both risk-aversion coefficients through strategic coupling. Specifically, the best-response system is*

$$\begin{cases} a_1^*(t) = \dfrac{\eta_1 e^{-\bar{r}(T-t)}}{\gamma_1\sigma_1^2} + \kappa_1\rho_{12}\dfrac{\sigma_2}{\sigma_1}a_2^*(t), \\ b_1^*(t) = \dfrac{m e^{-\bar{r}(T-t)}}{\gamma_1} - \dfrac{\sigma_v\rho_{\mathrm{sv}}e^{-\bar{r}(T-t)}}{\gamma_1}\sum_{i=1}^{n}\hat{B}_i(t) + \kappa_1 b_2^*(t), \end{cases} \tag{128}$$

$$\begin{cases} a_2^*(t) = \dfrac{\eta_2 e^{-\bar{r}(T-t)}}{\gamma_2\sigma_2^2} + \kappa_2\rho_{12}\dfrac{\sigma_1}{\sigma_2}a_1^*(t), \\ b_2^*(t) = \dfrac{me^{-\bar{r}(T-t)}}{\gamma_2} - \dfrac{\sigma_v\rho_{\mathrm{sv}}e^{-\bar{r}(T-t)}}{\gamma_2}\sum_{i=1}^n \hat{B}_i(t) + \kappa_2 b_1^*(t), \end{cases} \tag{129}$$

and the corresponding equilibrium value functions are given by

$$\begin{cases} V_1(t,z_1,v) = e^{\bar{r}(T-t)}z_1 + \dfrac{1}{\gamma_1}\sum_{i=1}^n B_i(t)v_i + \dfrac{C_1(t)}{\gamma_1}, \\ V_2(t,z_2,v) = e^{\bar{r}(T-t)}z_2 + \dfrac{1}{\gamma_2}\sum_{i=1}^n B_i(t)v_i + \dfrac{C_2(t)}{\gamma_2}, \end{cases} \tag{130}$$

where $B_i(t)$ and $\hat{B}_i(t)$ are given by (107) *and* (105)*, while $C_k(t)$ is given by* (110)*.*

If an unconstrained retention falls outside $[0,1]$, the constrained equilibrium is the unique fixed point of the projected best responses

$$\begin{cases} a_1^*(t) = \mathrm{Proj}_{[0,1]}\left(\dfrac{\eta_1 e^{-\bar{r}(T-t)}}{\gamma_1\sigma_1^2} + \kappa_1\rho_{12}\dfrac{\sigma_2}{\sigma_1}a_2^*(t)\right), \\ a_2^*(t) = \mathrm{Proj}_{[0,1]}\left(\dfrac{\eta_2 e^{-\bar{r}(T-t)}}{\gamma_2\sigma_2^2} + \kappa_2\rho_{12}\dfrac{\sigma_1}{\sigma_2}a_1^*(t)\right). \end{cases} \tag{131}$$

The product of the two cross-response slopes is $\kappa_1\kappa_2\rho_{12}^2 < 1$, so composition of the two projected responses is a contraction. Equation (131) therefore covers both lower and upper retention boundaries. The closed forms in (132) apply only when this fixed point is interior. The projected case is verified separately in Proposition 2.

Solving the two linear systems (128)–(129) explicitly gives the closed-form equilibrium strategies

$$\begin{cases} a_1^*(t) = \dfrac{\left[\frac{\eta_1}{\gamma_1\sigma_1^2} + \kappa_1\rho_{12}\frac{\eta_2}{\gamma_2\sigma_1\sigma_2}\right]e^{-\bar{r}(T-t)}}{1-\kappa_1\kappa_2\rho_{12}^2}, \\ a_2^*(t) = \dfrac{\left[\frac{\eta_2}{\gamma_2\sigma_2^2} + \kappa_2\rho_{12}\frac{\eta_1}{\gamma_1\sigma_1\sigma_2}\right]e^{-\bar{r}(T-t)}}{1-\kappa_1\kappa_2\rho_{12}^2}, \end{cases} \tag{132}$$

and

$$\begin{cases} b_1^*(t) = \dfrac{e^{-\bar{r}(T-t)}}{1-\kappa_1\kappa_2}\left[\dfrac{m-\sigma_v\rho_{\mathrm{sv}}\sum_{i=1}^n\hat{B}_i(t)}{\gamma_1} + \kappa_1\dfrac{m-\sigma_v\rho_{\mathrm{sv}}\sum_{i=1}^n\hat{B}_i(t)}{\gamma_2}\right], \\ b_2^*(t) = \dfrac{e^{-\bar{r}(T-t)}}{1-\kappa_1\kappa_2}\left[\dfrac{m-\sigma_v\rho_{\mathrm{sv}}\sum_{i=1}^n\hat{B}_i(t)}{\gamma_2} + \kappa_2\dfrac{m-\sigma_v\rho_{\mathrm{sv}}\sum_{i=1}^n\hat{B}_i(t)}{\gamma_1}\right]. \end{cases} \tag{133}$$

Proof. For the affine candidates (97)–(98),

$$V_{k,z} = A, \qquad V_{k,v_i} = \frac{B_i}{\gamma_k}, \qquad g_{k,z} = \hat{A}, \qquad g_{k,v_i} = \frac{\hat{B}_i}{\gamma_k},$$
$$V_{k,zz} = V_{k,zv_i} = g_{k,zz} = g_{k,zv_i} = g_{k,v_iv_\ell} = 0. \tag{134}$$

Therefore

$$D_k := V_{k,zz} - \gamma_k(g_{k,z})^2 = -\gamma_k\hat{A}^2(t) < 0. \tag{135}$$

For fixed rival controls, the Hessian of the control-dependent part of the extended HJB expression is

$$\begin{pmatrix} \partial^2_{a_k a_k} & \partial^2_{a_k b_k} \\ \partial^2_{b_k a_k} & \partial^2_{b_k b_k} \end{pmatrix} = D_k \begin{pmatrix} \sigma_k^2 & 0 \\ 0 & \nu_n(t, \boldsymbol{\nu}) \end{pmatrix}. \tag{136}$$

It is negative definite on $\{\nu_n > 0\}$. Hence the first-order conditions (91)–(92) give the unique interior best response. At $\nu_n = 0$, the investment quadratic term vanishes. Equation (133) then specifies a continuous selection, but it does not imply uniqueness of the investment maximizer on that boundary.

Substitution of the affine derivatives into (93)–(94) and collection of the coefficients of z give

$$A'(t) + \bar{r}A(t) = 0, \qquad \hat{A}'(t) + \bar{r}\hat{A}(t) = 0, \qquad A(T) = \hat{A}(T) = 1, \tag{137}$$

whence $A(t) = \hat{A}(t) = e^{\bar{r}(T-t)}$. The coefficient of the factor vector in the conditional-mean equation is

$$\widehat{\boldsymbol{B}}'(t) - \left[D_n + (\kappa + m\sigma_v\rho_{\mathrm{sv}})\boldsymbol{c}\mathbf{1}^\top\right]\widehat{\boldsymbol{B}}(t) = -m^2\boldsymbol{c}, \qquad \widehat{\boldsymbol{B}}(T) = \mathbf{0}, \tag{138}$$

which is (104). Thus

$$\widehat{\boldsymbol{B}}(t) = m^2 \int_t^T e^{-M_g(s-t)}\boldsymbol{c}\,\mathrm{d}s. \tag{139}$$

The coefficient of the factor vector in the value equation is, similarly,

$$\boldsymbol{B}'(t) - (D_n + \kappa\boldsymbol{c}\mathbf{1}^\top)\boldsymbol{B}(t) = -\boldsymbol{c}R(t), \qquad \boldsymbol{B}(T) = \mathbf{0}, \tag{140}$$

which has the integral solution in (107). Since $\widehat{\boldsymbol{B}}$ is unique, R is uniquely determined; hence $\boldsymbol{B}$ is unique. The remaining scalar coefficients satisfy

$$C_k'(t) = -C_k(t), \qquad \hat{C}_k'(t) = -\widehat{C}_k(t), \qquad C_k(T) = \hat{C}_k(T) = 0. \tag{141}$$

Their unique solutions are the integrals displayed after (109). Therefore the affine pair solves both equations of the extended HJB system.

To solve the coupled first-order conditions, set

$$\begin{aligned} \alpha_k(t) &:= \frac{\eta_k e^{-\bar{r}(T-t)}}{\gamma_k\sigma_k^2}, \qquad p_1 := \kappa_1\rho_{12}\frac{\sigma_2}{\sigma_1}, \qquad p_2 := \kappa_2\rho_{12}\frac{\sigma_1}{\sigma_2}, \\ h(t) &:= m - \sigma_v\rho_{\mathrm{sv}}\sum_{i=1}^n \hat{B}_i(t), \qquad \beta_k(t) := \frac{e^{-\bar{r}(T-t)}h(t)}{\gamma_k}. \end{aligned} \tag{142}$$

Equations (128)–(129) are equivalent to

$$\begin{pmatrix} 1 & -p_1 \\ -p_2 & 1 \end{pmatrix}\begin{pmatrix} a_1^* \\ a_2^* \end{pmatrix} = \begin{pmatrix} \alpha_1 \\ \alpha_2 \end{pmatrix}, \qquad \begin{pmatrix} 1 & -\kappa_1 \\ -\kappa_2 & 1 \end{pmatrix}\begin{pmatrix} b_1^* \\ b_2^* \end{pmatrix} = \begin{pmatrix} \beta_1 \\ \beta_2 \end{pmatrix}. \tag{143}$$

Their determinants are

$$\Delta_a = 1 - p_1p_2 = 1 - \kappa_1\kappa_2\rho_{12}^2 > 0, \qquad \Delta_b = 1 - \kappa_1\kappa_2 > 0. \tag{144}$$

Consequently,

$$\begin{pmatrix} a_1^* \\ a_2^* \end{pmatrix} = \frac{1}{\Delta_a} \begin{pmatrix} 1 & p_1 \\ p_2 & 1 \end{pmatrix} \begin{pmatrix} \alpha_1 \\ \alpha_2 \end{pmatrix}, \qquad \begin{pmatrix} b_1^* \\ b_2^* \end{pmatrix} = \frac{1}{\Delta_b} \begin{pmatrix} 1 & \kappa_1 \\ \kappa_2 & 1 \end{pmatrix} \begin{pmatrix} \beta_1 \\ \beta_2 \end{pmatrix}. \tag{145}$$

These two identities are exactly (132)–(133). The assumed interiority makes the retention maximizers feasible. The displayed affine candidates extend to $C^{1,2}$ functions on $[0, T) \times \mathbb{R}^{n+2}$, and their generator identities are polynomial in ν_n; by continuity, the identities also hold when $\nu_n = 0$. Proposition 1 and Assumption 1 verify the admissibility and integrability hypotheses of Theorem 2; applying that theorem proves the stated time-consistent Nash equilibrium. The displayed affine coefficient system and its interior best-response solution are unique.

Proposition 2. *Suppose that Assumption 1 holds and $\kappa_1\kappa_2 < 1$. Let (a_1^*, a_2^*) be the projected fixed point in* (131)*, let (b_1^*, b_2^*) be given by* (133)*, and use the continuous investment selection when $\nu_n = 0$. Define B_i, $\hat{B}_i$, C_k, and $\hat{C}_k$ as above, with the projected retentions substituted directly in both* (108) *and* (109)*. Then the affine candidates satisfy the constrained extended HJB system, and the resulting profile is a time-consistent Nash equilibrium of the finite-factor game. The projected-retention system has a unique fixed point. At $\nu_n = 0$, the investment Hamiltonian is constant in b_k, and* (133) *provides the continuous admissible investment selection.*

Proof. Fix t and a rival retention a_j. Up to terms independent of a_k, the retention-dependent HJB expression is

$$\Phi_k(a_k; a_j) = \frac{D_k\sigma_k^2}{2} a_k^2 + \left(\eta_k V_{k,z} - D_k\kappa_k\rho_{12}\sigma_k\sigma_j a_j\right) a_k, \qquad 0 \le a_k \le 1. \tag{146}$$

Since $D_k = -\gamma_k \hat{A}^2 < 0$,

$$\Phi_k''(a_k; a_j) = D_k\sigma_k^2 < 0. \tag{147}$$

Its unconstrained maximizer is

$$\widehat{a}_k(a_j) = -\frac{\eta_k V_{k,z}}{D_k\sigma_k^2} + \kappa_k\rho_{12}\frac{\sigma_j}{\sigma_k} a_j = \frac{\eta_k e^{-\bar{r}(T-t)}}{\gamma_k\sigma_k^2} + \kappa_k\rho_{12}\frac{\sigma_j}{\sigma_k} a_j. \tag{148}$$

Strict concavity therefore gives

$$\arg\max_{a_k \in [0,1]} \Phi_k(a_k; a_j) = \mathrm{Proj}_{[0,1]}(\widehat{a}_k(a_j)). \tag{149}$$

Define

$$T_1(x) := \mathrm{Proj}_{[0,1]}\left(\frac{\eta_1 e^{-\bar{r}(T-t)}}{\gamma_1\sigma_1^2} + \kappa_1\rho_{12}\frac{\sigma_2}{\sigma_1} x\right), \tag{150}$$

$$T_2(x) := \mathrm{Proj}_{[0,1]}\left(\frac{\eta_2 e^{-\bar{r}(T-t)}}{\gamma_2\sigma_2^2} + \kappa_2\rho_{12}\frac{\sigma_1}{\sigma_2} x\right). \tag{151}$$

Projection onto $[0, 1]$ is nonexpansive. Hence, for $x, y \in [0, 1]$,

$$\left|T_1(T_2(x)) - T_1(T_2(y))\right| \le \kappa_1\kappa_2\rho_{12}^2 |x - y|. \tag{152}$$

Since $\kappa_1\kappa_2\rho_{12}^2 < 1$, Banach's theorem gives a unique fixed point a_1^* of $T_1 \circ T_2$; putting $a_2^* = T_2(a_1^*)$ gives the unique solution of (131).

The projected retentions depend only on time. Thus they enter (93)–(94) only in the constant terms, and

$$\widehat{\boldsymbol{B}}' = M_g\widehat{\boldsymbol{B}} - m^2\boldsymbol{c}, \qquad \boldsymbol{B}' = (D_n + \kappa\boldsymbol{c}\mathbf{1}^\top)\boldsymbol{B} - \boldsymbol{c}R \tag{153}$$

remain unchanged, with the same terminal conditions. The remaining coefficients are obtained directly from (108)–(109) after substitution of the projected controls. This step is necessary because an interior retention first-order condition cannot be used at a boundary.

For investment, the second derivative of the HJB expression is $D_k\nu_n$. It is strictly negative on $\{\nu_n > 0\}$, so its first-order conditions give (133). When $\nu_n = 0$, the investment Hamiltonian is constant in b_k, and the continuous value in (133) is an admissible selection. Hence the projected retentions maximize the constrained retention problem, and the selected investments maximize the investment problem on the interior. The affine candidates satisfy the extended HJB equations on the whole viable state set, including $\nu_n = 0$, by their $C^{1,2}$ extensions and continuity. Assumption 1 and Proposition 1 verify the hypotheses of Theorem 2, which yields the stated time-consistent Nash equilibrium.

Table 1. Baseline parameter values for the numerical experiments.

Parameter	Symbol	Value
Risk-free rate	r_f	0.05
Effective accumulation rate	$\bar{r}$	0.047619
Delay decay rate and horizon	δ, h	0.10, 1
Memory normalization	q_δ	1.050833
Memory loading	χ	0.05
Distributed- and point-delay weights	α, β	0.007381, 0.047542
Planning horizon	T	5
Number of factors	n	8
Truncation interval	$[\underline{\eta}, \overline{\eta}]$	[0.01, 50]
Hurst index	H	0.10
Vol-of-vol	σ_v	1.0
Variance mean-reversion	κ	0.5
Initial and long-run variance	v_0, ω	0.04, 0.04
Stock–variance correlation	ρ_{sv}	−0.7
Variance-risk premium	m	0.3
Relative-concern (both insurers)	κ_1, κ_2	0.5
Insurer–insurer risk correlation	ρ_{12}	0.3
Insurer 1: reins. prem., claim vol., risk aversion	$\eta_1, \sigma_1, \gamma_1$	0.12, 0.40, 1.0
Insurer 2: reins. prem., claim vol., risk aversion	$\eta_2, \sigma_2, \gamma_2$	0.12, 0.35, 1.5
Factor rates $\gamma_{n,i}$ (baseline $H = 0.10$)		0.169, 1.117, 3.321, 7.103, 12.731, 20.437, 30.428, 42.896
Factor weights $c_{n,i}$ (baseline $H = 0.10$)		approximately 0.4374 for each i; unrounded sum 3.4990

5. Numerical experiments

The numerical experiments quantify the model-implied mechanisms in (132)–(133). Throughout, the rough variance is represented by the finite-factor model in Section 3. The rates $\gamma_{n,i}$ and weights $c_{n,i}$ are obtained from an equal-mass partition of the rough-kernel moment measure in (31), following [31]. For $H = 0.10$, $n = 8$, and $[\underline{\eta}, \overline{\eta}] = [0.01, 50]$, the rates lie in $[0.169, 42.896]$, each weight is approximately 0.4374, and the unrounded sum is $\sum_i c_{n,i} = 3.4990$.

The delay parameters are selected jointly. Given $r_f = 0.05$, $\delta = 0.10$, $h = 1$, and $\chi = 0.05$, the normalization constant is $q_\delta = 1.050833$, and we impose both compatibility relations used in the state reduction:

$$\beta = \chi q_\delta e^{-\delta h} = 0.047542, \qquad \alpha = \frac{\chi(\delta + r_f - \beta + \chi q_\delta)}{1 + \chi} = 0.007381. \tag{154}$$

Consequently, $\bar{r} = r_f - \alpha - \beta + \chi q_\delta = 0.047619$, and the transformed wealth process is consistent with the original delayed dynamics. The remaining values in Table 1 provide a transparent numerical benchmark. The choices $H = 0.10$ and $\rho_{\mathrm{sv}} = -0.7$ are selected on the basis of the rough-volatility evidence in [29] and determine the model-implied equilibrium strategies reported below.

Table 2. Kernel and strategy stability across factor discretizations. The strategy-error reference is the 128-factor grid; zero strategy errors in that row are by construction, whereas both kernel errors are measured against the fractional kernel. The Time and Hurst columns report E_b^{time} and E_b^{Hurst}, respectively, in percent.

n	$[\underline{\eta}, \overline{\eta}]$	$L^2[0,T]$	$L^2[0.01,T]$	Time	Hurst	Peak H
8	$[0.01, 50]$	45.93	23.39	3.91	7.30	0.198
16	$[0.01, 50]$	44.79	20.03	3.05	7.12	0.183
32	$[0.01, 50]$	44.52	19.18	2.83	7.08	0.178
32	$[0.005, 100]$	40.61	14.36	1.87	5.12	0.203
64	$[0.001, 200]$	36.62	7.43	0.41	1.36	0.245
128	$[0.0005, 400]$	33.95	5.54	0.00	0.00	0.259

Approximation-error and convergence assessments. Table 2 reports kernel error on both the theorem-relevant interval $[0, T]$ and the truncated interval $[0.01, T]$. For an interval I,

$$E_K(I) = 100 \frac{\|K - K_n\|_{L^2(I)}}{\|K\|_{L^2(I)}}. \tag{155}$$

The integrals are evaluated by adaptive Gauss–Kronrod quadrature. To define the two strategy-stability columns, let

$$\mathcal{T} = \{0, 0.005, \ldots, 5\}, \qquad \mathcal{H} = \{0.05, 0.051, \ldots, 0.45\}. \tag{156}$$

The time-profile error uses the baseline Hurst index $H = 0.10$ and is

$$E_b^{\mathrm{time}}(n) = 100 \frac{\max_{t \in \mathcal{T}} \left| b^*_{1,n}(t; 0.10) - b^*_{1,128}(t; 0.10) \right|}{\max_{t \in \mathcal{T}} \left| b^*_{1,128}(t; 0.10) \right|}. \tag{157}$$

The Hurst-sensitivity error compares initial investment over the Hurst grid,

$$E_b^{\mathrm{Hurst}}(n) = 100\frac{\max_{H\in\mathcal{H}}\left|b^*_{1,n}(0;H) - b^*_{1,128}(0;H)\right|}{\max_{H\in\mathcal{H}}\left|b^*_{1,128}(0;H)\right|}. \tag{158}$$

The peak column reports $H_n^{\mathrm{peak}} = \arg\max_{H\in\mathcal{H}} b^*_{1,n}(0;H)$. The 128-factor row is only an internal numerical reference. Its nonzero kernel error shows that it is not the limiting rough solution. Near-zero kernel singularity materially increases the full-interval error. The Hurst peak also moves from 0.198 to 0.259, so its location is not numerically stable and is not assigned economic significance. The strategy-error columns measure agreement with the 128-factor reference only and are not error bounds relative to the limiting rough model.

The notation keeps distinct the claim-risk correlation ρ_{12}, which enters retention, and the stock–variance correlation ρ_{sv}, which enters investment. Likewise, κ denotes variance mean-reversion, whereas κ_k denotes insurer k's relative-performance concern. The matrix M_g in (103) records aggregate-drift and hedging feedback couplings. Cross-factor second-order covariations instead enter the generator through the common variance Brownian motion and enter $R(t)$ through squared factor sums. The factor coefficients are therefore not independent scalar solutions, but the two coupling mechanisms remain distinct.

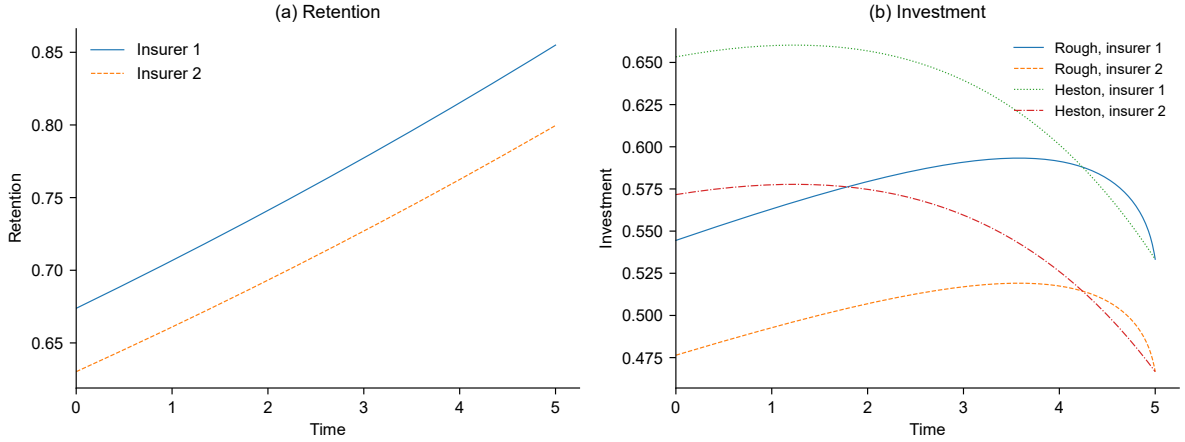


Figure 1. Baseline equilibrium strategies over time. Insurer 1 is shown by a blue solid line and insurer 2 by an orange dashed line. (a) Retention $a_k^*(t)$; (b) rough and standard-Heston investment $b_k^*(t)$ in monetary units. The Heston retention curves coincide with the rough curves and are not plotted separately. All undisplayed parameters are fixed at Table 1.

Baseline profiles. Figure 1 displays the equilibrium strategies for both insurers. The reinsurance retention $a_k^*(t)$ increases towards maturity: $a_1^*(t)$ moves from 0.674 to 0.855, and $a_2^*(t)$ from 0.630 to 0.800. This time pattern is determined by $e^{-\bar{r}(T-t)}$ in (132), the delay-induced effective accumulation factor. Investment is mildly hump-shaped: $b_1^*(t)$ rises from 0.544 to 0.593 at $t \approx 3.58$ and then falls to 0.533, while $b_2^*(t)$ rises from 0.476 to 0.519 and ends at 0.467. The hump combines the mean–variance term $me^{-\bar{r}(T-t)}/\gamma_k$, the volatility-hedging term, and strategic coupling. Since $\widehat{\boldsymbol{B}}(T) = \mathbf{0}$, the hedging term vanishes at maturity, and investment converges to $m(1/\gamma_k + \kappa_k/\gamma_j)/(1-\kappa_1\kappa_2)$. The standard-Heston benchmark $K(t) = 1$, represented by one factor with $c_1 = 1$ and $\gamma_{n,1} = 0$, leaves retention unchanged but

raises initial investment to 0.653 and 0.572 for insurers 1 and 2. Both Heston investment curves meet the rough curves at maturity because the volatility-hedging coefficient vanishes there. Insurer 1 invests more than insurer 2 throughout, which reflects its lower risk-aversion level $\gamma_1 < \gamma_2$.

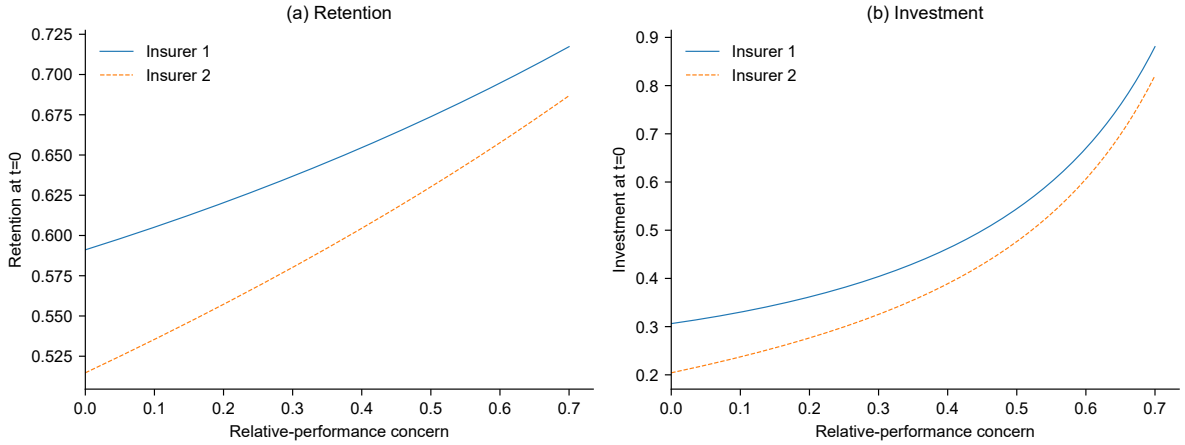


Figure 2. Sensitivity of the initial equilibrium strategies to the relative-concern coefficient $\kappa = \kappa_1 = \kappa_2$ over $[0, 0.7]$. Insurer 1 is blue solid and insurer 2 orange dashed. (a) Initial retention; (b) initial investment in monetary units.

Relative-performance concern. Figure 2 displays the initial strategies as $\kappa_1 = \kappa_2 = \kappa$ varies from 0 to 0.7. As κ grows, retention rises from 0.591 to 0.717 for insurer 1 and from 0.515 to 0.687 for insurer 2. Investment rises from 0.306 to 0.881 and from 0.204 to 0.821, respectively. These responses have different denominators: Retention contains $1 - \kappa_1\kappa_2\rho_{12}^2$, whereas investment contains $1 - \kappa_1\kappa_2$. Thus the larger investment response in this range is determined by the two distinct best-response systems. At $\kappa = 0$, both systems reduce to their no-relative-concern benchmarks.

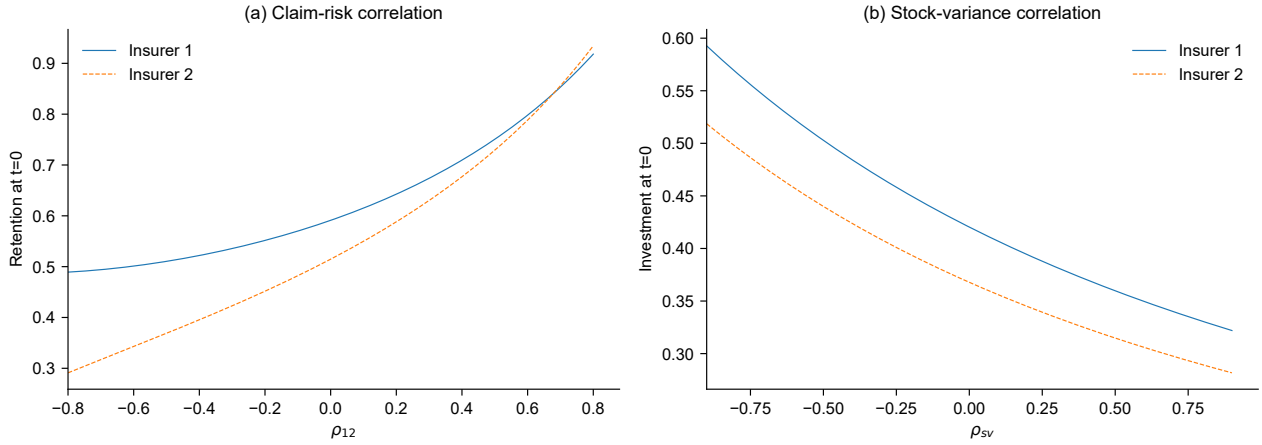


Figure 3. Sensitivity to the two correlation structures (evaluated at $t = 0$). (a) Reinsurance retention $a_k^*(0)$ versus the insurer–insurer risk correlation ρ_{12}. (b) Investment $b_k^*(0)$ versus the stock–variance correlation ρ_{sv}. Insurer 1 is blue solid and insurer 2 orange dashed; all other parameters are fixed at Table 1.

The two correlation channels. Figure 3 varies the two correlations separately. In panel (a), the reinsurance strategy is plotted against the insurer–insurer risk correlation ρ_{12}. Increasing ρ_{12} from -0.8 to 0.8 lifts the initial retention from 0.489 to 0.918 for insurer 1 and from 0.291 to 0.934 for insurer 2. This is the cross-response channel in (132); investment does not contain ρ_{12}. In panel (b), increasing ρ_{sv} from -0.9 to 0.9 reduces initial investment from 0.593 to 0.322 for insurer 1 and from 0.519 to 0.282 for insurer 2. For this parameterization, negative stock–variance correlation raises the volatility-hedging component. Retention does not contain ρ_{sv}. These comparative statics show that the closed-form equilibrium assigns ρ_{12} to retention and ρ_{sv} to the volatility-hedging component of investment.

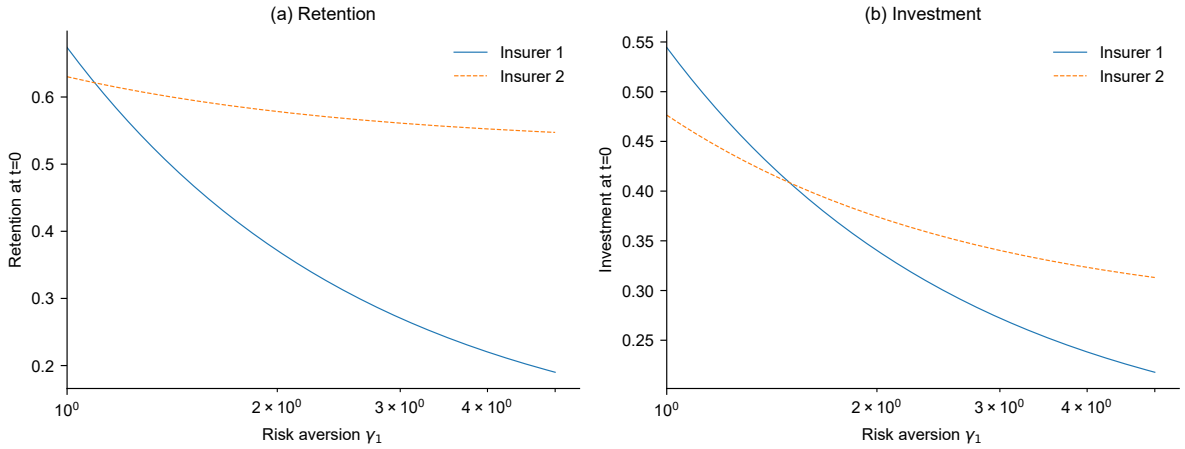


Figure 4. Sensitivity of the initial equilibrium strategies to insurer 1's risk-aversion coefficient $\gamma_1 \in [1, 5]$ (log scale on the horizontal axis, $\gamma_2 = 1.5$ fixed). Insurer 1 is blue solid and insurer 2 orange dashed. (a) Retention; (b) investment in monetary units.

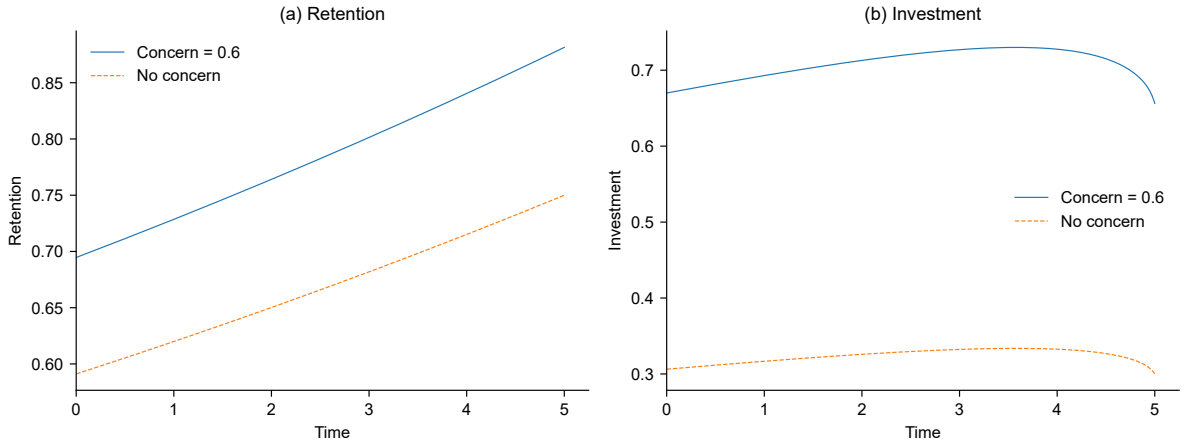


Figure 5. Equilibrium strategies of insurer 1 with relative-performance concern $\kappa = 0.6$ (solid) and without concern $\kappa = 0$ (dashed). (a) Retention; (b) investment in monetary units. Other parameters are fixed at Table 1.

Risk aversion. Figure 4 reports the initial strategies as insurer 1's risk-aversion coefficient γ_1 varies from 1 to 5 on a logarithmic scale (with $\gamma_2 = 1.5$ fixed). Raising γ_1 from 1 to 5 reduces its retention

from 0.674 to 0.190 and its investment from 0.544 to 0.218. Insurer 2 responds through the strategic cross terms: Its retention falls from 0.630 to 0.547 and its investment from 0.476 to 0.313. The own response is larger than the spillover under the baseline parameters.

Game and no-concern benchmark. Figure 5 contrasts the full game ($\kappa = 0.6$) with the standard no-concern economy ($\kappa = 0$). Relative-performance concern raises both controls for the displayed parameters. At $t = 0$, insurer 1's retention changes from 0.591 to 0.695 and investment from 0.306 to 0.670; at T, retention changes from 0.750 to 0.881 and investment from 0.300 to 0.656. This comparison isolates the effect of the strategic cross terms while holding the market, delay, and preference parameters fixed. It does not impose or infer a financing link between the two controls.

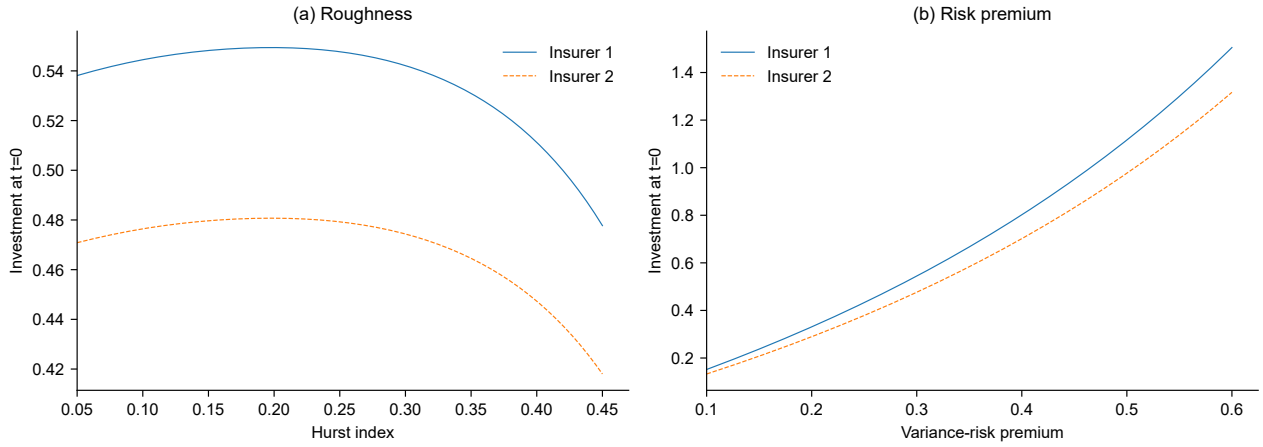


Figure 6. Sensitivity of the initial investment strategy to the volatility specification. (a) Hurst index H; (b) variance-risk premium m. Insurer 1 is blue solid and insurer 2 orange dashed. The Hurst panel uses the baseline eight-factor rule separately at each H; Table 2 reports the associated stability check.

Roughness and the variance-risk premium. Figure 6 plots the initial investment against the Hurst index H in panel (a) and against the variance-risk premium m in panel (b). The eight-factor response to H is mildly non-monotone: Insurer 1's investment rises from 0.538 at $H = 0.05$ to approximately 0.549 near $H = 0.20$ and then falls to 0.478 at $H = 0.45$; insurer 2 moves from 0.471 to approximately 0.481 and then to 0.418. Changing H changes the full quadrature and the coupled hedging coefficient. Table 2 shows that the non-monotone shape persists on richer grids and that its peak location changes across grids. The reported Hurst response is characterized by the range of initial investments over the specified grid. In panel (b), increasing m from 0.1 to 0.6 raises investment from 0.152 to 1.505 for insurer 1 and from 0.133 to 1.317 for insurer 2. These results quantify the model-implied response to the variance-risk premium under the reported baseline parameterization.

Delay-memory sensitivity. Finally, Figure 7 varies χ over $[0, 0.20]$ while recomputing $\beta = \chi q_\delta e^{-\delta h}$ and $\alpha = \chi(\delta + r_f - \beta + \chi q_\delta)/(1 + \chi)$. This joint recomputation preserves both compatibility conditions at every point. As χ increases, $\bar{r}$ declines from 0.0500 to 0.0417. Initial retention rises from 0.666 to 0.694 for insurer 1 and initial investment from 0.538 to 0.561; insurer 2 has the same directional

response. At $\chi = 0$, compatibility gives $\alpha = \beta = 0$ and $\bar{r} = r_f$, so the left endpoint of each delay curve is exactly the literal no-delay economy. The dotted horizontal lines are the literal no-delay economy $\chi = \alpha = \beta = 0$, shown separately for the two insurers. The open-circle and open-square benchmarks are independently recomputed no-memory economies with $\chi = \alpha = \beta = 0$ and with the risk-free rate set equal to the corresponding delayed effective rate $\bar{r}$ at each value of χ. The matched-rate controls coincide exactly with the compatible-delay controls because (132)–(133) transmit the delay parameters to the controls through $\bar{r}$. Delay also changes the terminal criterion and value through the state transformation $\bar{Z}_k = Z_k + \chi Y_k$.

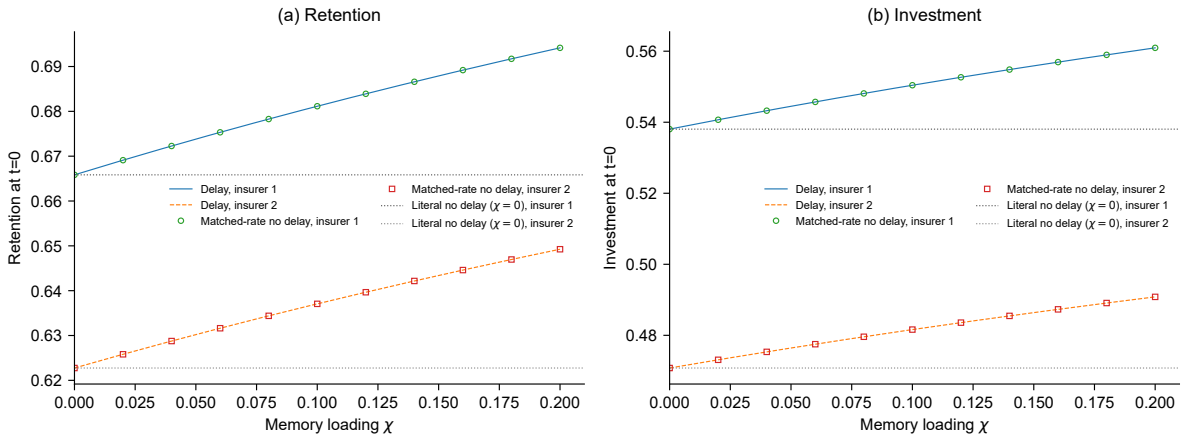


Figure 7. Sensitivity of the initial strategies to the memory loading χ along the compatible delay-parameter path. Insurer 1 is blue solid and insurer 2 orange dashed. Open circles mark the matched-effective-rate no-delay control for insurer 1; open squares show the independently recomputed matched-effective-rate no-delay control for insurer 2. Both marker series coincide with their corresponding delay curves. Dotted horizontal lines show the respective literal no-delay benchmarks. (a) Retention; (b) investment in monetary units.

6. Conclusions

This paper formulates a time-consistent mean–variance reinsurance–investment game for two insurers with normalized delayed wealth and a multifactor approximation of rough Heston volatility. A compatibility condition produces a finite-dimensional sufficient statistic for a restricted delay subclass. The joint feedback state and viable forward-variance cone clarify the domain of the finite-factor game. The verification argument uses explicit fourth-moment, localization, domination, and uniform-integrability conditions. Transfer to the original rough game is only a conditional compact-action implication. Kernel convergence must be accompanied by state, payoff, and uniform local-gain stability.

The closed forms separate two strategic channels. Retention depends on the claim-risk correlation ρ_{12} and has denominator $1 - \kappa_1\kappa_2\rho_{12}^2$; investment depends on the stock–variance correlation ρ_{sv} and has denominator $1 - \kappa_1\kappa_2$. Thus the two controls do not share a common amplification factor. The volatility-hedging coefficient is determined by a coupled matrix system and vanishes at maturity. This first-order matrix coupling is distinct from the common-driver cross-factor second-order covariations, which enter the generator and $R(t)$ separately. The explicit solution is unique within the affine interior best-response

system. The numerical experiments respect the delay compatibility conditions, distinguish r_f from $\bar{r}$, and report finite-factor stability. The standard-Heston comparison isolates the rough-volatility hedging effect. The matched-rate no-delay comparison shows that the compatible-delay controls coincide with the matched-rate controls because the delay parameters enter through $\bar{r}$. Delay changes the transformed terminal criterion and value. Full-interval kernel errors and the grid-dependent Hurst peak characterize the numerical approximation, and the calculations quantify the model-implied equilibrium effects under the reported baseline parameterization.

By characterizing the joint role of reinsurance and investment in risk sharing, return generation, and solvency management, the results clarify how these two control channels interact in a competitive insurance market.

Extensions to more insurers, constrained investment, ambiguity, transaction costs, or model uncertainty require new equilibrium and verification arguments. Empirical estimation of both the loss-memory parameters and the rough-volatility specification will support quantitative assessment of the reported numerical magnitudes.

Author contributions

Yong He: Conceptualization, methodology, supervision, validation, and writing–review and editing. Ga Ba: Methodology, formal analysis, software, visualization, and writing–original draft. Both authors read and approved the final manuscript.

Use of Generative-AI tools declaration

During revision, the authors used OpenAI Codex to assist with language editing, reference-format harmonization, DOI verification, and LaTeX typesetting. The tool was not used to generate research data, perform the mathematical derivations, conduct the numerical analyses, or draw scientific conclusions. The authors reviewed and verified all AI-assisted changes and take full responsibility for the content of the manuscript.

Conflict of interest

The authors declare no conflict of interest.

References

1. H. Markowitz, Portfolio selection, *J. Finance,* **7** (1952), 77–91. https://doi.org/10.1111/j.1540-6261.1952.tb01525.x
2. D. Li, W. L. Ng, Optimal dynamic portfolio selection: Multiperiod mean-variance formulation, *Math. Finance,* **10** (2001), 387–406. https://doi.org/10.1111/1467-9965.00100
3. X. Zhou, D. Li, Continuous-time mean-variance portfolio selection: A stochastic LQ framework, *Appl. Math. Optim.,* **42** (2000), 19–33. https://doi.org/10.1007/s002450010003
4. R. C. Merton, Optimum consumption and portfolio rules in a continuous-time model, *J. Econ. Theory,* **3** (1971), 373–413. https://doi.org/10.1016/0022-0531(71)90038-X

5. T. Björk, M. Khapko, A. Murgoci, On time-inconsistent stochastic control in continuous time, *Finance Stoch.,* **21** (2017), 331–360. https://doi.org/10.1007/s00780-017-0327-5
6. T. Björk, A. Murgoci, X. Zhou, Mean-variance portfolio optimization with state-dependent risk aversion, *Math. Finance,* **24** (2014), 1–24. https://doi.org/10.1111/j.1467-9965.2011.00515.x
7. Y. Zeng, Z. Li, Optimal time-consistent investment and reinsurance policies for mean-variance insurers, *Insur. Math. Econom.,* **49** (2011), 145–154. https://doi.org/10.1016/j.insmatheco.2011.01.001
8. L. Bai, H. Zhang, Dynamic mean-variance problem with constrained risk control for the insurers, *Math. Methods Oper. Res.,* **68** (2008), 181–205. https://doi.org/10.1007/s00186-007-0195-4
9. G. Guan, Z. Liang, Optimal reinsurance and investment strategies for insurer under interest rate and inflation risks, *Insur. Math. Econom.,* **55** (2014), 105–115. https://doi.org/10.1016/j.insmatheco.2014.01.007
10. A. Bensoussan, C. C. Siu, S. C. P. Yam, H. Yang, A class of non-zero-sum stochastic differential investment and reinsurance games, *Automatica,* **50** (2014), 2025–2037. https://doi.org/10.1016/j.automatica.2014.05.033
11. L. Bian, Y. Shen, W. Zhang, B. Zou, Mean-variance investment and reinsurance optimization with stochastic interest rate and volatility, *Quant. Finance,* **25** (2025), 1615–1637. https://doi.org/10.1080/14697688.2025.2566353
12. W. Jiang, X. Huang, Heston model about optimal investment and proportional reinsurance strategies for an insurer, *Braz. J. Probab. Stat.,* **39** (2025), 151–164. https://doi.org/10.1214/25-BJPS628
13. S. Basak, A. Pavlova, A. Shapiro, Optimal asset allocation and risk shifting in money management, *Rev. Financ. Stud.,* **20** (2007), 1583–1621. https://doi.org/10.1093/rfs/hhm026
14. G. E. Espinosa, N. Touzi, Optimal investment under relative performance concerns, *Math. Finance,* **25** (2015), 221–257. https://doi.org/10.1111/mafi.12034
15. C. C. Siu, S. C. P. Yam, H. Yang, H. Zhao, A class of nonzero-sum investment and reinsurance games subject to systematic risks, *Scand. Actuar. J.,* **2017** (2017), 670–707. https://doi.org/10.1080/03461238.2016.1228542
16. C. Deng, X. Zeng, H. Zhu, Non-zero-sum stochastic differential reinsurance and investment games with default risk, *Eur. J. Oper. Res.,* **264** (2018), 1144–1158. https://doi.org/10.1016/j.ejor.2017.06.065
17. S. Basak, G. Chabakauri, Dynamic mean-variance asset allocation, *Rev. Financ. Stud.,* **23** (2010), 2970–3016. https://doi.org/10.1093/rfs/hhq028
18. Y. Yang, G. Wang, J. Yao, Time-consistent reinsurance-investment games for multiple mean-variance insurers with mispricing and default risks, *Insur. Math. Econom.,* **114** (2024), 79–107. https://doi.org/10.1016/j.insmatheco.2023.11.004
19. C. Zhang, Z. Liang, Q. Li, Time-consistent investment and reinsurance strategies under thinning-dependence structure, *IMA J. Manag. Math.,* **36** (2025), 833–859. https://doi.org/10.1093/imaman/dpaf011
20. J. Guo, X. Han, H. Wang, K. C. Yuen, A nonzero-sum game with reinforcement learning under mean-variance framework, *ASTIN Bull.,* **56** (2026), 154–180. https://doi.org/10.1017/asb.2025.10080

21. H. Zhu, M. Cao, C. Zhang, Time-consistent investment and reinsurance strategies for mean-variance insurers with relative performance concerns under the Heston model, *Finance Res. Lett.,* **30** (2019), 280–291. https://doi.org/10.1016/j.frl.2018.10.009
22. N. Wang, N. Zhang, Z. Jin, L. Qian, Robust non-zero-sum investment and reinsurance game with default risk, *Insur. Math. Econom.,* **84** (2019), 115–132. https://doi.org/10.1016/j.insmatheco.2018.09.009
23. N. Wang, N. Zhang, Z. Jin, L. Qian, Reinsurance-investment game between two mean-variance insurers under model uncertainty, *J. Comput. Appl. Math.,* **382** (2021), 113095. https://doi.org/10.1016/j.cam.2020.113095
24. L. Li, H. Mi, Optimal investment and consumption with stochastic factor and delay, *ANZIAM J.,* **61** (2019). https://doi.org/10.21914/anziamj.v61i0.13011
25. M. Arriojas, Y. Hu, S. E. Mohammed, G. Pap, A delayed Black and Scholes formula, *Stoch. Anal. Appl.,* **25** (2007), 471–492. https://doi.org/10.1080/07362990601139669
26. G. Zhou, Z. Qiu, S. Li, A hybrid reinsurance-investment game with delay and asymmetric information, *J. Comput. Appl. Math.,* **440** (2024), 115491. https://doi.org/10.1016/j.cam.2023.115491
27. X. Han, D. Li, Y. Yuan, Robust reinsurance contract and investment with delay under mean-variance framework, *Commun. Stat. Theory Methods,* **53** (2024), 8614–8658. https://doi.org/10.1080/03610926.2023.2282380
28. G. Zhou, Q. Zhang, L. Zhong, Robust reinsurance and investment strategies with bounded memory in a stochastic Stackelberg differential game, *J. Ind. Manag. Optim.,* **21** (2025), 6760–6793. https://doi.org/10.3934/jimo.2025148
29. J. Gatheral, T. Jaisson, M. Rosenbaum, Volatility is rough, *Quant. Finance,* **18** (2018), 933–949. https://doi.org/10.1080/14697688.2017.1393551
30. O. El Euch, M. Rosenbaum, The characteristic function of rough Heston models, *Math. Finance,* **29** (2019), 3–38. https://doi.org/10.1111/mafi.12173
31. E. Abi Jaber, O. El Euch, Multifactor approximation of rough volatility models, *SIAM J. Financ. Math.,* **10** (2019), 309–349. https://doi.org/10.1137/18M1170236
32. E. Abi Jaber, Lifting the Heston model, *Quant. Finance,* **19** (2019), 1995–2013. https://doi.org/10.1080/14697688.2019.1615113
33. N. Bäuerle, S. Desmettre, Portfolio optimization in fractional and rough Heston models, *SIAM J. Financ. Math.,* **11** (2020), 240–273. https://doi.org/10.1137/18M1217243
34. A. Bondi, S. Pulido, S. Scotti, The rough Hawkes Heston stochastic volatility model, *Math. Finance,* **34** (2024), 1197–1241. https://doi.org/10.1111/mafi.12432
35. E. Motte, D. Hainaut, Partial hedging in rough volatility models, *SIAM J. Financ. Math.,* **15** (2024), 601–652. https://doi.org/10.1137/23M1583090



AIMS Press

© 2026 the Author(s), licensee AIMS Press. This is an open access article distributed under the terms of the Creative Commons Attribution License (https://creativecommons.org/licenses/by/4.0)